Natural Coordinates of Space and Time, Implied Quanta and Gravity and Structuring Applications in Geoinformatics

HANS-OTTO CARMESIN
University Bremen
Fachbereich 1 for Physics and Electrical Engineering, Otto-Hahn-Alle 1, 28359 Bremen
GERMANY
and
Studienseminar Stade
Bahnhofstr. 5, 21682 Stade and Gymnasium and Observatory Athenaeum ,
Harsefelder Str. 40, 21680 Stade
GERMANY

Abstract: Foucault discovered, that a coordinate system, that describes nature adequately, cannot rotate in an arbitrary manner. Similarly, Einstein and the International Astronomical Union (IAU) searched for the translatory motion of the coordinate systems that describe nature adequately. Indeed, the IAU proclaimed the problem of finding adequate coordinate systems. Such a coordinate system is very useful in space navigation, geoinformatics, and the prediction of physical properties. Such natural coordinates are tools that describe space and time in an adequate and predictive manner. The natural coordinates are discovered here by two independent methods: observation and derivation. Moreover, natural coordinates are tools that imply quanta, gravity, and essential properties of time.

Key–Words: adequate coordinate system, geoinformatics, fluctuations, gravity, quantum physics, relativity, space navigation, space paradox, time, twin paradox, unification, universal absolute zero.

Received: November 30, 2025. Revised: January 3, 2026. Accepted: January 7, 2026.. Published: January 8, 2026.

1 Introduction

Space flight is essential for the exploration of space, celestial bodies, planets and Earth, see e. g. Lavery (1972); Starker et al. (1985); Soffel (2003); Riess (2022). Thereby, space navigation is an important tool, see e. g. Ashby (2003); Formichella et al. (2021). For it, the synchronization of clocks is basic for the measurement of the light travel distance, see Zogg (2009); Condon and Mathews (2018). For that purpose, time dilation, see Einstein (1905, 1915), and a 'nature describing coordinate system', see Einstein (1916), or an 'adequate coordinate system (ACS)' are foundational, see the International Astronomical Union (IAU) Soffel (2003), Carmesin (2025e,c).

In this paper, the problem of finding an ACS (see section 2) is presented first. Secondly, three solutions are progressively derived: an empirical solution (see section 3), a general classical solution (see sections 4 and 4.3), and four emergent solutions (see sections 6, 7, 8, 9). Thirdly, structuring applications to geoinformatics and to the Artemis Moon mission are elaborated (see sections 11 and 12). Fourthly, the results are concluded and critically discussed (see section 14).

The structure of the paths of derivation in this paper are illustrated in Fig. (20).

2 Problem of finding an adequate coordinate system for space and time

2.1 First foundation of an ACS

Already in ancient times, the question arose, whether Earth or Sun is in the center of our planetary system, see Hoskin (1999), Aristarchos (270). Today, geometrical, mechanical and optical empirical evidence shows that Sun is at the center, see Galileo (1638), Sardin (2001), Foucault (1851). Accordingly, since ancient times, the world has been described with help of numbers and coordinate systems, as mathematical tools, see Hoskin (1999), Archimedes (1897), Aristarchos (270). Correspondingly, the question arose whether the coordinate system that describes nature adequately moves with Earth, or whether it moves with Sun.

Here and in the following, the coordinate system that describes nature adequately is called adequate coordinate system (ACS). Thereby, the name 'coordinate system that describes nature' has been used by Einstein in modern times, see Einstein (1916), and the name 'adequate coordinate system' has been used by the IAU in modern times, see Soffel (2003). Both names mean the same.

The first mechanical and empirical foundation of an essential property of an ACS has been provided by Foucault with his pendulum, see Foucault (1851) and Fig. (1): The plane in which a Foucault pendulum

Figure 1: A Foucault pendulum in the Pantheon in Paris.

swings at Earth's north pole is at rest relative to an inertial coordinate system, according to Galileo's principle of inertia, see Galileo (1638), Newton (1687), Landau and Lifschitz (1960). Consequently, an ACS does not rotate around Earth's axis relative to such a Foucault pendulum. Therefore, for each ACS near Earth, that Foucault pendulum determines the angular frequency of the rotation around Earth's axis.

2.2 Proposed coordinate system

Einstein proposed that all conceivable coordinate systems should be regarded as equivalent for the description of nature, see Einstein (1916), p. 776, lines 5-17: [1] *'The only possibility is to assume that all conceivable coordinate systems can be used for the description of nature with equal legitimation, in principle. This means the following requirement: The general laws of nature must be expressed by equations, that hold for all coordinate systems, i. e. that are covariant with respect to arbitrary substitutions. It is clear that a physical science that fulfills this postulate, obeys the postulate of general relativity. As all substitutions include all relative motions of three-dimensional coordinate systems.'* See (Einstein, 1916, p. 776, lines 5-17).

This proposal is very idealized, as Foucault did already provide a founded restriction for a coordinate system that describes nature, see Foucault (1851), Shech (2023), Song (2002). Accordingly, this proposal is hardly sufficient for space navigation, see section (2.3). As a consequence, the problem proposed by the IAU is essential, to find an ACS that is useful for space navigation, see Soffel (2003).

2.3 Insufficiency of the proposed coordinate system for space navigation

The IAU realized that the coordinate system proposed by present - day relativity theory is insufficient for space navigation. Accordingly, the IAU proposed the 'problem of defining a useful and adequate coordinate system in astronomy', see Soffel (2003), p. 2688, column 2, lines 7-8. For the communication in the physics community, this problem has alternatively been called 'frame problem', see Carmesin (2025e).

2.4 Efficient summary of time dilation

In this section, the *equation of time dilation* of general relativity theory (GRT) is derived. This includes the equation of kinematic time dilation of special relativity theory (SRT). Thereby, that equation is derived progressively for various useful cases and in corresponding forms. In particular, that equation is derived for the case of a relatively slow ($v/c \ll 1$) clock C in a relatively small absolute value of the potential ($2|\Phi|/c^2 \ll 1$). Basically, that equation of time dilation is based on the scalar product that Einstein Einstein (1916) proposed in his Eq. 3:

$$ds^2 := \sum_{i=0}^{i=3} \sum_{j=0}^{j=3} g_{ij} dx_i dx_j \qquad (1)$$

This is an invariant with respect to transformations of the coordinate system. Hereby, the increment $dx_0 = c \cdot dt$ describes the distance that light propagates during an increment dt, whereby dt describes a coordinate time, describing a flat spacetime. Similarly, the increments dx_1, dx_2 and dx_3 describe the spatial coordinates in a flat spacetime. Thereby, the numbers g_{ij} are the elements of the metric tensor. Moreover, in GRT, ds^2 is a short notation for $(ds)^2$, or dx_j^2 is a short notation for $(dx_j)^2$, see e. g. Hobson et al. (2006).

[1] 'Es bleibt daher nichts anderes übrig, als alle denkbaren Koordinatensysteme als für die Naturbeschreibung prinzipiell gleichberechtigt anzusehen. Dies kommt auf die Forderung hinaus: Die allgemeinen Naturgesetze sind durch Gleichungen auszudrücken, die für alle Koordinatensysteme gelten, d. h. die beliebigen Substitutionen gegenüber kovariant (allgemein kovariant) sind. Es ist klar, dass eine Physik, welche diesem Postulat genügt, dem allgemeinen Relativitätspostulat gerecht wird. Denn in allen Substitutionen sind jedenfalls auch diejenigen enthalten, welche allen Relativbewegungen der (dreidimensionalen) Koordinatensysteme entsprechen.' See (Einstein, 1916, p. 776, lines 5-17).

Without loss of generality, we choose a locally orthogonal coordinate system. As a consequence, the scalar product in Eq. (1) has the following form

$$ds^2 = \sum_{j=0}^{j=3} g_{jj} dx_j^2 = g_{00} \cdot c^2 \cdot dt^2 - \sum_{j=1}^{j=3} |g_{jj}| dx_j^2. \quad (2)$$

In a typical analysis in GRT, a clock C is considered. In the coordinate system or reference system of the clock C, the time increment measured by the clock is named $d\tau$, and the spatial increments are zero, $d\xi_1 = 0$, $d\xi_2 = 0$ and $d\xi_3 = 0$. Consequently, the scalar product ds^2 is equal to $c^2 d\tau^2$,

$$ds^2 = c^2 d\tau^2 \quad \text{in a clock's coordinate system} \quad (3)$$

Of course, the usual GRT and SRT notation with τ for a system with a clock is hardly specific by itself. The notation can be made specific in a context.

As a further consequence, the squared time increment $d\tau^2$ in the coordinate system of a clock C in Eq. (3) is transformed to the squared time increment dt^2 in an *external coordinate system* (with respect to the clock C) in Eq. (2) by using the invariance of ds^2:

$$c^2 d\tau^2 = ds^2 = g_{00} \cdot c^2 \cdot dt^2 - \sum_{j=1}^{j=3} |g_{jj}| dx_j^2. \quad (4)$$

In order to solve for $d\tau^2$, the above Eq. is divided by c^2. Moreover, the above sum is multiplied by $1 = \frac{dt^2}{dt^2}$, and $\sum_{j=1}^{j=3} |g_{jj}| dx_j^2/dt^2$ is identified with the squared velocity of the clock C in the external coordinate system. As a consequence, the squared time measured by the clock C has the following form

$$d\tau^2 = dt^2 \cdot \left(g_{00} - \sum_{j=1}^{j=3} |g_{jj}| \frac{dx_j^2}{dt^2} \frac{1}{c^2} \right) = dt^2 \cdot \left(g_{00} - \frac{v^2}{c^2} \right). \quad (5)$$

In order to solve for $d\tau$, the square root is applied to the above Eq.

$$d\tau = dt \cdot \sqrt{g_{00} - \frac{v^2}{c^2}}. \quad (6)$$

In the case $v = 0$, there remains the gravitational time dilation:

$$d\tau_{grav} = dt \cdot \sqrt{g_{00}} \quad \text{or} \quad \frac{d\tau_{grav} - dt}{dt} = \sqrt{g_{00}} - 1. \quad (7)$$

Equation of time dilation in SRT: In the particular case of a flat spacetime, the tensor element g_{00} is one. As a consequence, the time $d\tau$ measured by a considered clock C in Eq. (6) has the form

$$d\tau = dt \cdot \sqrt{1 - \frac{v^2}{c^2}}, \quad \text{in flat spacetime.} \quad (8)$$

This term is identified with the equation of time dilation in special relativity theory, SRT, see Einstein (1905), Hobson et al. (2006). Minkowski (1908) explained this fact by realizing that SRT describes a flat spacetime, which is now called Minkowski space.

Equation of time dilation near a mass: Schwarzschild Schwarzschild (1916) derived the metric tensor elements g_{ij} that describe spacetime in the vicinity of an uncharged and non-rotating mass M. Thereby, at a coordinate distance r from M, the element g_{00} is

$$g_{00} = 1 - \frac{R_S}{r} \quad \text{with} \quad R_S = \frac{2GM}{c^2} \quad (9)$$

Hereby, R_S is named Schwarzschild radius, G is Newton's gravitational constant $G = 6.674\,30(15) \cdot 10^{-11}\ \frac{\mathrm{m}^3}{\mathrm{kg \cdot s}^2}$, and c is the velocity of light in vacuum, $c = 299\,792\,458\ \frac{\mathrm{m}}{\mathrm{s}}$, see Navas et al. (2024).

Equation of time dilation at a potential: In Newton's theory of gravitation, the gravitational potential at a coordinate r is as follows[2], see Karttunen et al. (2007):

$$\Phi(r) = -\frac{GM}{r}. \quad (10)$$

As a consequence, the tensor element g_{00} in Eq. (9) as a function of the potential in Eq. (10) is

$$g_{00} = 1 - \frac{2|\Phi|}{c^2}. \quad (11)$$

As a consequence, the time $d\tau$ measured by a considered clock C in Eq. (6) has the form

$$d\tau = dt \cdot \sqrt{1 - \frac{2|\Phi|}{c^2} - \frac{v^2}{c^2}}, \quad \text{near a mass.} \quad (12)$$

Equation for a slow clock in a small potential: In this section, equation (12) of time dilation is analyzed for a clock C that has a relatively small velocity v with

[2]This term has also been derived in an exact theory of gravity, in which distances are determined according to the local curvature of spacetime, see Carmesin (2025e).

respect to the external coordinate system, and that is in a relatively small absolute value of the potential $|\Phi|$,

$$\frac{v}{c} \ll 1, \quad \text{and} \quad \frac{2|\Phi|}{c^2} \ll 1. \tag{13}$$

For instance, these conditions are fulfilled for vehicles including space crafts that travel in our planetary system, in the vicinity of Earth or on Earth. As a consequence of the condition in Eq. (13), the root in equation (12) of time dilation can be expanded at linear order, marked by $\doteq$,

$$d\tau \doteq dt - dt \cdot \frac{|\Phi|}{c^2} - dt \cdot \frac{v^2}{2c^2}. \tag{14}$$

In equation (14) of time dilation, the subtrahends are identified with the gravitational time difference $d\tau_{grav}$ and the kinematic time difference $d\tau_{kin}$,

$$d\tau \doteq dt + d\tau_{grav} + d\tau_{kin}, \quad \text{with}$$
$$d\tau_{grav} = -dt \cdot \frac{|\Phi|}{c^2}, \quad \text{and} \quad d\tau_{kin} = -dt \cdot \frac{v^2}{2c^2}. \tag{15}$$

The above time increments are divided by the increment of the coordinate time dt,

$$\frac{d\tau}{dt} \doteq 1 + \delta\tau_{grav,frac} + \delta\tau_{kin,frac}, \quad \text{with}$$
$$\delta\tau_{grav,frac} = -\frac{|\Phi|}{c^2} = \frac{\Phi}{c^2}, \quad \text{and}$$
$$\delta\tau_{kin,frac} = -\frac{v^2}{2c^2}. \tag{16}$$

Hereby, $\delta\tau_{grav,frac} := \frac{d\tau_{grav}}{dt}$ and $\delta\tau_{kin,frac} := \frac{d\tau_{kin}}{dt}$ are called gravitational fractional time difference and kinematic fractional time difference. The time difference and the fractional time difference are

$$\delta t = d\tau - dt \implies \frac{\delta t}{dt} = \frac{d\tau}{dt} - 1 \quad \text{and}$$
$$\delta\tau_{frac} := \frac{\delta t}{dt} = \delta\tau_{grav,frac} + \delta\tau_{kin,frac}. \tag{17}$$

Next, these equations of time differences are applied in order to derive the ACS.

2.5 Paradoxical nature of the proposed coordinate system: twin paradox

In order to draw the attention to the question of a coordinate system that describes space and time of nature in an adequate manner, Langevin proposed the twin paradox, Langevin (1911). This can be summarized by the following scenario:

The twins Nele and Deike celebrate their 15^{th} birthday. Nele travels for $\Delta t_{nele} = 6$ a, six years, with a speed $|\vec{v}| = v = 0.8 \cdot c$. Deike stays at Earth at a place with a negligible gravity and velocity. If the Earth Centered Inertial (ECI) coordinate system is used, which is at rest at Earth and at a Foucault pendulum at the north pole, then, Deike's age increases by a factor $\frac{5}{3}$ faster than Nele's age. Consequently, Deike's age increased by $\Delta t_{Deike} = \frac{5}{3} \cdot \Delta t_{Nele} = 10$ a, 10 years, according to Eq. (8).

However, according to the coordinate systems proposed by Einstein (see section), it should be equivalent to choose a coordinate system that is at rest at Nele's spacecraft. In that coordinate system, Nele is at rest, and Deike moves at the velocity $|\vec{v}| = v = 0.8 \cdot c$. Consequently, in that coordinate system, Deike's age increased by $\Delta t_{Deike} = \frac{3}{5} \cdot \Delta t_{Nele} = 3.6$ a, 3.6 years, according to Eq. (8).

As Deike's age cannot increase by 3.6 years and by 10 years simultaneously, this result is paradox. This paradox is called twin paradox. It is solved next in an empirical manner.

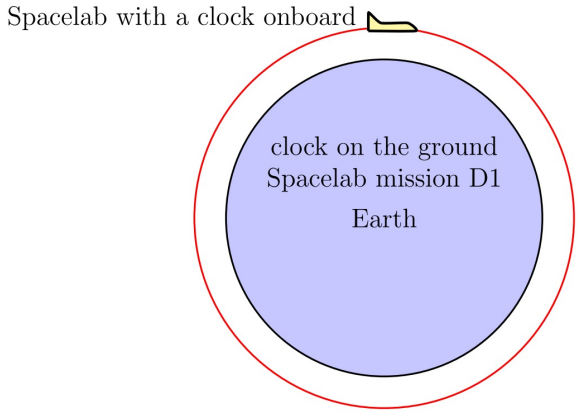

Figure 2: Observation of time dilation: In the Spacelab mission D1, a clock in the orbit has been compared with a clock on the ground.

3 Empirical solution

A shuttle experiment has been performed on the Spacelab mission D1, in order to investigate the gravitational and kinematic time dilation or time difference, see Starker et al. (1982), Starker et al. (1985) and Fig. (2).

For it, the Spacelab traveled in a circular orbit around Earth. Thereby, the Spacelab had the planned altitude $h_{Sh} = 325$ km above the ground, see Starker et al. (1982), figure 19. In a DFVLR (1985) Report, the altitude $h_{Sh} = 324$ km is reported. In summary,

$$h_{Sh} = 324 \pm 1 \text{ km} \tag{18}$$

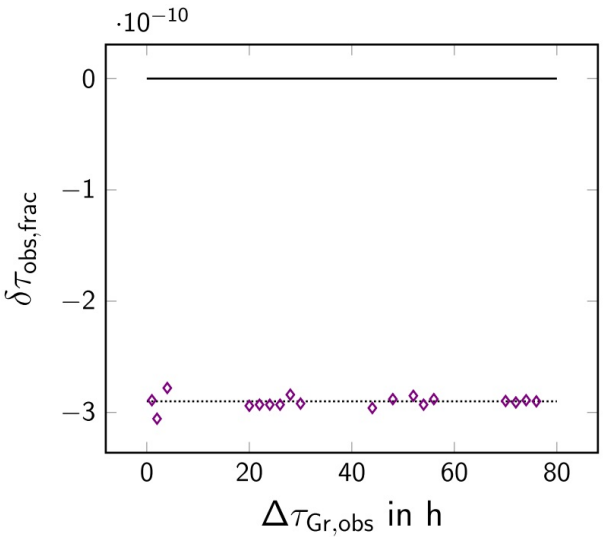

Figure 3: Observed fractional time difference $\delta\tau_{obs,frac} = \frac{\Delta\tau_{Sh,obs}-\Delta\tau_{Gr,obs}}{\Delta\tau_{Gr,obs}}$ as a function of the time $\Delta\tau_{Gr,obs}$ elapsed at the ground. As a result, $\delta\tau_{obs,frac}$ is a negative constant.

The ground station was Oberpfaffenhofen. Its height above sea level is $H_{Ober} = 580(\pm 20)$ m, see Starker et al. (1982), figure 19. The uncertainty (± 20), as well as its latitude $\beta_{Ober} = 48.0813889^o$ are taken from geographic maps. From it, the radial coordinate is calculated, see Ashby (2003), Eq. (20):

$$\begin{aligned} r = a_0 + a_2x^2 + a_4x^4 + a_6x^6 + a_8x^8, \text{ with} \\ x = \sin(90^o - \beta_{Ober}), \text{ and} \\ a_0 = 6356742.025; a_2 = 21353.642; \\ a_4 = 39.832; a_6 = 0.798; a_8 = 0.003 \\ \text{thus, } r = 6\,366\,280.658 \text{ m} \end{aligned} \quad (19)$$

As a consequence, the orbital radius R_{orbit} is equal to the above radius r of the ground station, plus the height H_{Ober}, plus the height above the ground

$$\begin{aligned} R_{orbit} = r + H_{Ober} + h_{Sh} \\ = 6\,690\,280.658(\pm 1020) \text{ m} \end{aligned} \quad (20)$$

Consequently, the orbital velocity is

$$\begin{aligned} v_{orbit} = \sqrt{\frac{GM_E}{R_{orbit}}} \\ = 7\,718.745(\pm 1)\ \frac{\text{m}}{\text{s}}, \end{aligned} \quad (21)$$

with $GM_E = 3.986\,004\,418 \cdot 10^{14}\ \frac{\text{N}\cdot\text{m}^2}{\text{kg}}$.

In a clock experiment of the D1 mission, the Spacelab had two atomic clocks onboard, a Cs-clock and a Rb-clock. Equal clocks were placed on the ground in Oberpfaffenhofen, Germany. The clocks were compared by one-way and two-way methods, see Starker et al. (1985).

3.1 Observation

First results showed that the onboard clocks exhibit an observed fractional time difference compared to the clocks on the ground, see figure 5 in Starker et al. (1985) and figure (3):

$$\begin{aligned} \delta t_{obs,frac} = \delta t_{obs,frac,Sh} - \delta t_{obs,frac,Gr} \\ = -2.968(\pm 0.198) \cdot 10^{-10} \end{aligned} \quad (22)$$

3.2 Derivation

In this section, the observation is compared with the derived result. Hereby, the following ACS is used: Firstly, an Earth centered ACS is used, as the IAU recommended a Geocentric Celestial Reference System (GCRS) for space flight in Earth's vicinity, see Soffel (2003). Secondly, the ACS should not rotate around Earth's axis relative to the plane of a Foucault pendulum at the north pole, according to Foucault's discovery, see Foucault (1851). Altogether, the Earth Centered Inertial coordinate system (ECI) is used as the ACS in a founded manner.

The fractional gravitational time difference at the Shuttle is as follows:

$$\begin{aligned} \delta\tau_{grav,frac,Sh} : \doteq -\frac{GM_E}{c^2 R_{orbit}} \\ = -6.629\,06\,(\pm 0.000\,97) \cdot 10^{-10} \end{aligned} \quad (23)$$

The fractional kinematic time difference of the onboard clocks is

$$\begin{aligned} \delta\tau_{kin,frac,Sh} : \doteq -\frac{v_{orbit}^2}{2 \cdot c^2} \\ = -3.314\ 53\,(\pm 0.000\ 49) \cdot 10^{-10}. \end{aligned} \quad (24)$$

At the ground, the angular frequency ω_{ECI} relative to the ECI is 2π divided by the sidereal day:

$$\omega_{ECI} = \frac{2\pi}{86164.09\text{ s}} = 7.292\,116 \cdot 10^{-5}\ \frac{1}{\text{s}} \quad (25)$$

Consequently, at the ground station at the radius $r = 6366.280$ km, the kinematic fractional time difference is

$$\begin{aligned} \delta\tau_{kin,frac,Gr} \doteq -\frac{\omega_{ECI}^2 \cdot r^2}{2c^2} \\ = -1.199\,186(\pm 0.000\,0076) \cdot 10^{-12}. \end{aligned} \quad (26)$$

At the ground, the fractional gravitational time difference is

$$\begin{aligned} \delta\tau_{grav,frac,Gr} : \doteq -\frac{GM_E}{c^2 \cdot r} \\ = -6.967\,034(\pm 0.000\,0178) \cdot 10^{-10}. \end{aligned} \quad (27)$$

The derived fractional time difference of the time at the shuttle minus the time at the ground is as follows:

$$\begin{aligned}\delta\tau_{derived,frac} &= \delta\tau_{kin,frac,Sh} + \delta\tau_{grav,frac,Sh} \\ &\quad -(\delta\tau_{kin,frac,Gr} + \delta\tau_{grav,frac,Gr}) \\ &= -2.904\,978(\pm 0.001\,508)\cdot 10^{-10} \end{aligned} \quad (28)$$

This result is in precise accordance with observation within the errors of measurement, see Eq. (22). This accordance confirms the theory that is formed by the equations of relativity together with the used ACS, the ECI.

3.3 Empirical solution of the twin paradox

The observation in Eq. (22) shows that there elapses more time at the clock on the ground than at the clock that moves above the ground. If this result is applied to the twin paradox in section (2, part 2.5), then it is predicted that there elapses more time at Deike's clock on the ground than at Nele's clock that moves relative to Earth's ground in space.

Though the empirical observation at the Spacelab in the D1 mission is very convincing, the observation is a particular case only. Accordingly, a general solution of the twin paradox would be essential in addition. This is derived in the next section (4).

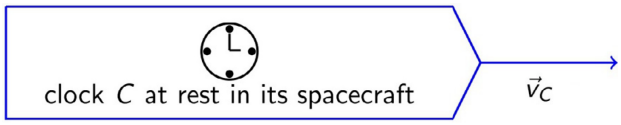

Figure 4: Spacecraft with a fixed onboard clock.

4 General classical solution

4.1 Measurement of the ACS

In this section, for each point P, an ACS is identified. While the ACS is a physically based coordinate system, an arbitrary conventional reference system is used as a tool. Similarly, in order to express the physically based absolute temperature with its Kelvin Kelvin (1848) scale, the conventional Celsius scale is used: zero Kelvin equals minus 273.15 degree Celsius.

Conventional reference system: In general, each point P can be located relative to one or more celestial bodies. These celestial bodies are used as an arbitrary conventional reference system, CS. Additionally, a clock at the conventional reference system can be used as a reference. Hereby, in general, P can move relative to the conventional reference system. As a notation, a velocity of a clock C relative to the system CS is denoted by $\vec{v}_{C,\underline{CS}}$, or $\vec{v}_C$ for short, and a used coordinate system is marked by an underlined subscript.

Measurement of the velocity of the ACS: In this section, a method for the measurement of the velocity $\vec{v}_{ACS}$ of the ACS is presented. Thereby, that velocity $\vec{v}_{ACS,\underline{CS}}$ is described relative to the conventional reference system CS.

At each point P, the velocity $\vec{v}_{ACS,\underline{CS}}$ of the ACS can be measured as follows:

A spacecraft with an onboard clock C and a velocity $\vec{v}_C$ is used (see Fig. 4). When the spacecraft is at rest in the ACS, then the velocity $\vec{v}_C$ of the clock is equal to the velocity $\vec{v}_{ACS,\underline{CS}}$ of the ACS:

$$\vec{v}_{C,\underline{CS}} - \vec{v}_{ACS,\underline{CS}} = 0, \quad \text{iff C is at rest in the ACS.} \quad (29)$$

Hereby and as usual, iff abbreviates 'if and only if'. The above equation is transformed equivalently by application of the square and division by $-2c^2$:

$$-\frac{(\vec{v}_{C,\underline{CS}} - \vec{v}_{ACS,\underline{CS}})^2}{2c^2} = 0, \quad \text{iff C is at rest in the ACS.} \quad (30)$$

Moreover, when the spacecraft is at rest in the ACS, the law of kinematic time dilation holds, see Eq. (16) and Fig. (5):

$$\delta\tau_{kin,frac} = \frac{-(\vec{v}_{C,\underline{CS}} - \vec{v}_{ACS,\underline{CS}})^2}{2c^2} = 0, \quad \text{iff C is at rest in the ACS.} \quad (31)$$

In the above equation, the fraction is zero iff it takes its maximal value $\delta\tau_{kin,frac,max}$:

$$\delta\tau_{kin,frac} = \delta\tau_{kin,frac,max} = 0, \quad \text{iff C is at rest in the ACS.} \quad (32)$$

The above equation and statement are used for the measurement of $\vec{v}_{ACS,\underline{CS}}$ as follows: For each point P, a spacecraft, including another vehicle in a wider sense, with an onboard clock C is used, see Fig. (4). Thereby, the clock is at rest in the spacecraft. The spacecraft is moved so that the observed kinematic time difference of the clock C is maximal. This is tested by a permanent comparison with a clock at the conventional reference system. For it, a permanent radio transmission is used, whereby a possible Doppler effect is corrected. Moreover, the velocity $\vec{v}_{C,\underline{CS}}$ is measured (relative to the conventional reference system).

As a result, the spacecraft is at rest in the ACS. Consequently, the measured velocity $\vec{v}_{C,\underline{CS}}$ provides the velocity of the ACS (see Eq. 29):

$$\vec{v}_{ACS,\underline{CS}} = \vec{v}_{C,\underline{CS}}, \quad \text{as the clock C is at rest in the ACS.} \tag{33}$$

Altogether, this method can provide the ACS and its velocity in general, for each point P in the universe. More practical devices for that measurement are presented in Carmesin (2025e,f,g,h).

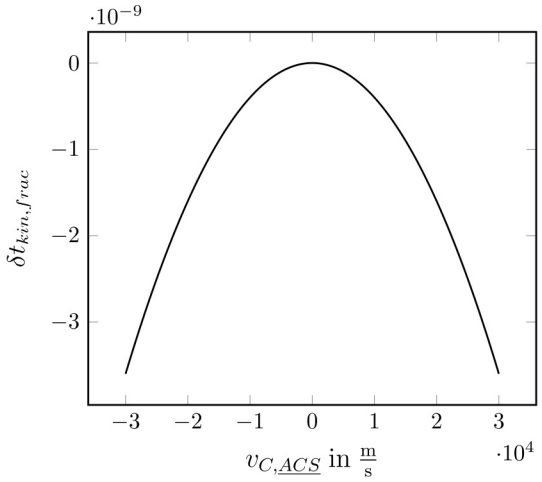

Figure 5: For each point P in the universe, and for each clock C near P, the kinematic fractional time difference $\delta t_{kin,frac}$ as a function of the speed $v_{C,\underline{ACS}}$ = $|\vec{v}_{C,\underline{CS}} - \vec{v}_{ACS,\underline{CS}}|$ relative to the adequate coordinate system ACS of P is shown. Everywhere in the universe, the maximum of $\delta t_{kin,frac}$ is zero at $v_{C,\underline{ACS}} = 0$, this holds when quantum fluctuations are ignored.

Existence & velocity-uniqueness of the ACS: For each point P, the quadratic equation in Eq. (31) has exactly one solution. Therefore, for each P, there exists an ACS. Moreover, the measured velocity $\vec{v}_{ACS,\underline{CS}}$ in Eq. (33) is uniquely determined, as any velocity of the spacecraft different from $\vec{v}_{ACS,\underline{CS}}$ would cause a kinematic time difference that is not maximal.

Therefore, the ACS exists and its velocity is determined in a unique manner.

Thus, the essential remaining question is: How can the velocity of the ACS be predicted?

4.2 Derivation of the ACS

In this section, a prediction of the velocity of the ACS is derived.

In general, at different points P_1 and P_2, the ACS has different velocities $\vec{v}_{ACS,\underline{CS}}(P_1) \neq \vec{v}_{ACS,\underline{CS}}(P_2)$. Therefore, even a fully screened clock onboard a spacecraft (see Fig. 4) must experience an interaction caused by its surroundings. Only with help of such an interaction, the clock can show the correct kinematic time difference, as this difference depends on the velocity of the ACS, see Eq. (31). As a consequence of the screening of the clock, the electromagnetic interaction, the weak interaction, and the strong interaction can be excluded, see Navas et al. (2024). Consequently, the clock must experience the gravitational interaction, which can be expressed in terms of the local gravitational field $\vec{G}^*(\vec{r})$. This vector field represents a pattern. Accordingly, the velocity that enters the equation of the kinematic time difference in Eq. (31) is the velocity relative to this pattern of the vector field $\vec{G}^*(\vec{r})$. (Alternatively, gravity can be expressed with help of curvature of spacetime or with help of additional volume, see Carmesin (2025e).)

In general, the field is moving. And a screened clock is at rest with all of its interaction with its surroundings, iff the clock is at rest at the field. Correspondingly, at each point P, the ACS is at rest at that pattern of the vector field $\vec{G}^*(\vec{r})$ at the point P, at which the ACS is determined.

For instance, in the vicinity of Earth, the vector field $\vec{G}^*(\vec{r})$ is at rest at the Earth Centered Inertial frame (ECI). Consequently, near Earth, the ACS is at rest at the ECI. This prediction has been confirmed by the Spacelab mission D1 in section (3) and Starker et al. (1985). Moreover, this prediction has been confirmed by other observations in space, see Carmesin (2025d,e), and by an observation at Earth, see Carmesin (2025c).

4.3 Universal zero of the kinematic time difference

In this section, an especially useful and insightful result is elaborated:

At each point P in the universe, there exists a measurable ACS with a measurable velocity $\vec{v}_{ACS,\underline{CS}}$.

Therefore, each clock C with its velocity $\vec{v}_{C,\underline{CS}}$ has the following kinematic fractional time difference, see Eq. (31):

$$\delta\tau_{kin,frac} = \frac{-(\vec{v}_{C,\underline{CS}} - \vec{v}_{ACS,\underline{CS}})^2}{2c^2} \tag{34}$$

Therefore, at each P, there is the absolute zero of the kinematic fractional time difference, $\delta\tau_{kin,frac} = 0$. It occurs for each clock C at P, that has the same velocity as the ACS, $\vec{v}_{C,\underline{CS}} = \vec{v}_{ACS,\underline{CS}}$. Thereby,

$\vec{v}_{ACS,\underline{CS}}$ is a function of P: The ACS is at rest at the local gravitational field at P. Accordingly, $\vec{v}_{ACS,\underline{CS}}(P)$ can be predicted, for more details see Carmesin (2025e). As a consequence, $\vec{v}_{ACS,\underline{CS}}$ can be used for space navigation and for the synchronization of clocks in a predictable manner. It is insightful to realize that the kinematic time difference is related to a local property of space and gravity, for more details see Carmesin (2025e). The absolute zero of the kinematic time difference represents a zero point of motion relative to the ACS. This is very valuable, as physical laws achieve a relatively clear structure and short form at the zero point of motion, for more details see Carmesin (2025e).

Moreover, the determination of the kinetic energy and of the relativistic energy of a clock C, i. e.

$$E = \frac{E_0}{\sqrt{1 - \vec{v}^2_{C,\underline{CS}}/c^2}} \tag{35}$$

become possible in a universal manner by using the velocity of the clock relative to the ACS, $\vec{v}_{C,\underline{CS}} = \vec{v}_{C,\underline{ACS}}$. This is the adequate term, as the relativistic energy can be derived from the term of the time dilation, see e. g. Hobson et al. (2006), Carmesin (2019, 2020); Burisch et al. (2025).

Furthermore, the plane, in which the Foucault pendulum swings, is at rest at Earth's gravitational field at a very high precision. The reason is that the frame dragging of Earth's gravitational field with Earth's rotation is extremely small, it is described by the Lense - Thirring effect, see Lense and Thirring (1918), Ciufolini and Pavlis (2004). Another reason is that gravitational fields of extraterrestrial celestial bodies are very small at Earth's surface.

5 Experiments with optical lattice clocks

The error of measurement of an optical lattice clock is very small. For instance, when the clock averages for one second, the error of measurement can be smaller than $\delta t_{frac} = 10^{-16}$, see Hinkley (2013). At long averaging, the precision can be $\delta t_{frac} = 3.5 \cdot 10^{-19}$, see Kim et al. (2023). With such clocks, the Einstein (1916) equivalence principle can be tested:

5.1 Test of the Einstein equivalence principle

Einstein (1916) proposed an Einstein equivalence principle, see Hobson et al. (2006), p. 149, lines 24-25, 'in a freely falling (non-rotating) laboratory occupying a small region of spacetime, the laws of physics are those of special relativity.' For instance, in space science, a freely falling capsule in a drop tower, see e. g. Joeris et al. (2025), can be regarded as such a freely falling non-rotating laboratory. According to the Einstein equivalence principle, the laws of special relativity theory should be applicable. In particular, the relativity principle should hold, so that kinematic time dilation should not be described by a special coordinate system. In contrast, Earth's ACS is at rest at Earth's gravitational field. Consequently, the ACS is the ECI at the drop tower. Therefore, this ACS is a special coordinate system. As a consequence, the capsule of the drop tower is falling relative to that coordinate system.

Thereby, at the Bremen drop tower, the capsule falls for $t = 4.74\,\mathrm{s}$, see Joeris et al. (2025). During that time, the capsule accelerates to the speed $v = g \cdot t = 46.5\ \frac{\mathrm{m}}{\mathrm{s}}$, relative to the ACS. Consequently, a clock in the capsule can measure the following kinematic time difference, during the last second:

$$\begin{aligned} \delta t_{kin,frac} &= \int_{3.74\,\mathrm{s}}^{4.74\,\mathrm{s}} \frac{g^2 \cdot t^2}{2c^2} dt \\ &= \left[\frac{g^2 \cdot t^3}{6c^2}\right]_{3.74\,\mathrm{s}}^{4.74\,\mathrm{s}} = 9.656 \cdot 10^{-15} \end{aligned} \tag{36}$$

Remind that this kinematic fractional time difference $9.656 \cdot 10^{-15}$ is based on a special coordinate system, the ECI. In contrast, in the Einstein Equivalence Principle, there is no special coordinate system. Consequently, in the Einstein Equivalence Principle, there is no way to predict the velocity $v = 46.5\ \frac{\mathrm{m}}{\mathrm{s}}$. Therefore, in the Einstein Equivalence Principle, there is no way to predict the kinematic fractional time difference $9.656 \cdot 10^{-15}$.

It should be possible to measure that kinematic fractional time difference $9.656 \cdot 10^{-15}$ with an optical lattice clock onboard the capsule. During the process of free fall, the optical lattice clock should not be disturbed and operate in a normal mode. At the touch down, the optical lattice clock might be disturbed. This should not influence the measurement, as this took place before the touch down. Consequently, this proposed test of the Einstein equivalence principle could be feasible.

5.2 Test of the ACS on Earth's ground

Grotti et al. (2024) measured the gravitational potential difference $\Delta\Phi$ between the Physikalisch - Technische Bundesanstalt (PTB) in Braunschweig and the Max Planck Institute for Quantum Optics (MPQ) in Garching. They used two measurement principles: A geodetic measurement provided a value $\Delta\Phi_g$, and a chronometric measurement with optical lattice clocks

with a precision of $\delta t_{frac} \approx 10^{-18}$ provided a value $\Delta\Phi_c$. The difference is in the following interval, see Carmesin (2025c):

$$\Delta\Phi_c - \Delta\Phi_g \in \left[-0.68 \frac{\mathrm{m}}{\mathrm{s}^2}; 5.12 \frac{\mathrm{m}}{\mathrm{s}^2}\right] \tag{37}$$

In the following, a used coordinate system (or frame) is marked by an underlined subscript. The circular frequency $\omega_{\oplus,\underline{ECI}}$ of Earth's rotation measured relative to the ECI is 2π divided by the periodic time of the sidereal day $d_{sid} = 86\,164.09\,\mathrm{s}$. The circular frequency $\omega_{\oplus,\underline{ACS}}$ of Earth's rotation measured relative to the ACS is measured on the basis of clocks. The interval of potential differences in Eq. (37) implies that $\omega_{\oplus,\underline{ACS}}$ is in the following interval, see Carmesin (2025c):

$$\omega_{\oplus,\underline{ACS}} \in \left[0.4138 \cdot \omega_{\oplus,\underline{ECI}}; 1.0535 \cdot \omega_{\oplus,\underline{ECI}}\right] \tag{38}$$

In this manner, a measurement on Earth's ground with optical lattice clocks provided a value for the motion $\omega_{\oplus,\underline{ACS}}$ of the ACS as a function of $\omega_{\oplus,\underline{ECI}}$. Within the error of measurement, this measurement confirms the IAU recommendation, see Soffel (2003), that the ECI should be used as an ACS in Earth's vicinity.

6 Emergent quantum solution

In this section, the quantum postulates are derived. This is achieved in the framework of the hypothetic deductive method. For it, basic and empirically founded properties of space and time are described in the following section, and these properties represent the very founded hypotheses in that framework:

6.1 Hypothetic deductive method I

In this paper, the results are obtained by the hypothetic deductive method, see Popper (1935, 1974), Niiniluoto et al. (2004). Hereby, the following hypotheses are used:

Used hypotheses: In this section, the hypotheses are presented that are used in the hypothetic deductive method. Thereby, these hypotheses are very founded. Therefore, the risk of failure is very small.

(1) The space, that can be observed in the whole volume V ranging from Earth to the light horizon, is isotropic and homogeneous at this universal scale. Local heterogeneities are possible, for instance near a mass M, see Schwarzschild (1916), Dyson et al. (1920), Pound and Rebka (1960). This has been observed, see Planck-Collaboration (2020).

(1.1) Moreover, there is natural space that is very homogeneous and isotropic at small scales. For instance, natural space is very homogeneous and isotropic in a void, see Zeldovich et al. (1982), Contarini et al. (2024), and natural space was very homogeneous and isotropic in the early universe, see Planck-Collaboration (2020).

(1.2) Furthermore, in the heterogeneous universe, natural space can exhibit slight heterogeneity, additionally. For instance, in the heterogeneous universe, Abbott et al. Abbott (2016) observed the merger of a binary stellar-mass black hole system, and the gravitational waves emitted thereby. These gravitational waves can be interpreted as coherent states that cannot be emitted in a natural homogeneous universe without heterogeneity, as only an appropriate heterogeneity can emit coherent states.

(2) Space has a positive energy density u_{DE}, it is the dark energy density. It is the density of the energy E of the volume V of the space in part (1), divided by this volume:

$$u_{DE} = \frac{E}{V}. \tag{39}$$

This has been discovered by Perlmutter et al. Perlmutter et al. (1998), see also Riess (2000), Smoot (2007).

(3) The energy speed relation of special relativity theory (SRT) holds, see Einstein (1905), Hobson et al. (2006): In general, an object with an energy E has a velocity $\vec{v}$ relative to a mass m_{ref}, that is used as a reference. Its absolute value is called speed $v = |\vec{v}|$. In the case of zero speed, $v = 0$, the energy is called rest energy E_0. The energy speed relation of SRT is as follows, see Eq. (35):

$$E_0^2 = E^2 \cdot \left(1 - \frac{v^2}{c^2}\right) \tag{40}$$

In the case $v < c$, the relation has the following equivalent form:

$$E^2 = \frac{E_0^2}{1 - \frac{v^2}{c^2}} \tag{41}$$

Hereby and in the following, the velocity is determined relative to an adequate coordinate system of relativity theory.

(4) Each volume or volume portion ΔV of space has zero rest energy E_0, and it has zero rest mass $m_0 = E_0/c^2$.

$$m_0(V) = 0 = E_0(V). \tag{42}$$

This is shown in the following paragraph.

(5) In a process of increase of volume or space, the dark energy density u_{DE} is a nonzero constant,

whereby only very small variations might occur. This approximate constancy has been observed for the expansion of space since the Big Bang, see Planck-Collaboration (2020), Riess (2022). Additionally, that constancy has been proposed by general relativity theory and cosmology, see Einstein (1917), Friedmann (1922), Lemaître (1927), Hobson et al. (2006). Furthermore, the value of u_{DE} is derived here, and the results are additional evidence for this approximate constancy.

The above very founded hypotheses (1) to (5) will be used for deductions in this paper.

Why volume has no rest mass: In this section, it is shown that volume has zero rest mass m_0.

In the vicinity of a mass M, there occurs additional volume δV, see Fig. (6). If that additional volume would have a rest energy $m_0(\delta V) > 0$, then there would be an additional rest mass m_0 in the vicinity of each mass M. Such an additional rest mass has never been observed, see e. g. Landau and Lifschitz (1976), Navas et al. (2024), Planck-Collaboration (2020), Zogg (2009). For instance, if there would be such an additional rest mass m_0, then this m_0 would modify the orbits of the GPS satellites, and this would have been observed, but this has not been observed. Consequently, additional volume δV has no rest mass.

Moreover, the additional volume in the vicinity of a mass is the same type of volume as the usual volume that occurs without any mass. This is confirmed by the observation that only one type of volume has been observed, see e. g. Navas et al. (2024), Planck-Collaboration (2020), Casimir (1948), Zeldovich (1968), Perlmutter et al. (1998). Therefore, in general, volume has no rest mass.

6.2 Space paradox

In general, a paradox provides the chance to develop a deep insight, see Brockhaus (1998). In this section, we will derive a paradox, and we will use it in order to develop a deep insight.

In the following, the space, that can be observed in the whole volume V ranging from Earth to the light horizon, is considered. For instance, this space has been observed, see Planck-Collaboration (2020).

In physical concepts that are commonly used at the present-day, the space with its volume V is considered as a *single entity*, see e. g. Newton (1687), Maxwell (1865), Einstein (1915), Friedmann (1922), Lemaître (1927), Landau and Lifschitz (1971), Hobson et al. (2006), Planck-Collaboration (2020).

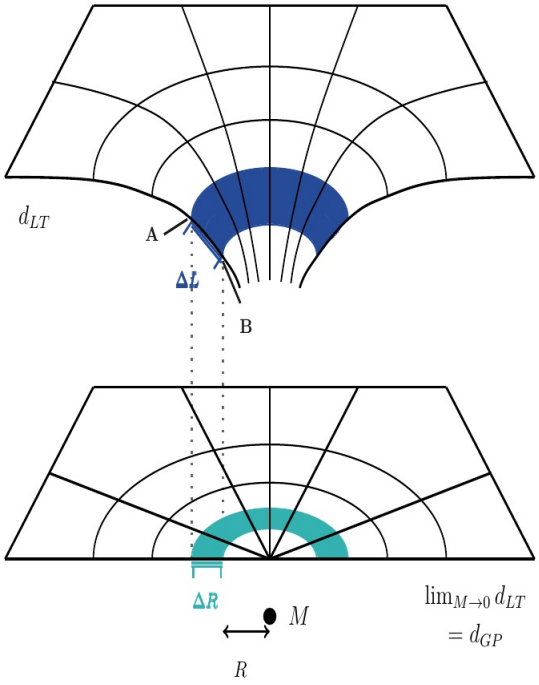

Figure 6: In the vicinity of a mass M, the radial difference ΔL is increased with respect to the original difference ΔR that would occur in the limit M to zero. Note that the difference ΔL is measured as a light travel distance d_{LT}, and the difference ΔR is measured as a gravitational parallax distance d_{GP}, see Carmesin (2021b, 2025e).

That space has a positive energy density u_{DE}, see Perlmutter et al. (1998):

$$u_{DE} = \frac{E}{V}. \tag{43}$$

As a consequence of SRT, the volume V with its energy E of space, velocity $\vec{v}$, and speed $|\vec{v}| = v$, obey the energy speed relation, see Eqs. (40 and 41)

$$E^2 = \frac{E_0^2}{1-\frac{v^2}{c^2}} \quad \text{or} \quad E^2 \cdot \left(1 - \frac{v^2}{c^2}\right) = E_0^2. \tag{44}$$

As the energy density is nonzero, the energy E is nonzero. Thus, the above relation can be divided by E^2. Therefore, the following form of the energy momentum relation holds:

$$1 - \frac{v^2}{c^2} = \frac{E_0^2}{E^2}. \tag{45}$$

As a consequence of the zero rest energy E_0 of V, see Eq. (42), the right hand side in Eq. (45) is zero. Consequently, the volume V with its energy E has the speed c of light in vacuum.

$$v = c = v(V) = v(E). \tag{46}$$

The paradox: In physical concepts that are commonly used at the present-day, the volume is considered as a single entity, see e. g. Newton (1687), Maxwell (1865), Einstein (1915), Friedmann (1922), Lemaître (1927), Landau and Lifschitz (1971), Hobson et al. (2006), Planck-Collaboration (2020). In such a concept of volume, that whole volume would move parallel to some unit direction vector $\vec{e}_v$ and with the speed of light, $\vec{v} = c \cdot \vec{e}_v$, see Eq. (46).

However, that velocity $\vec{v}$ would break the isotropy of space observed at a universal scale, see Planck-Collaboration (2020). This is a contradiction. In general, a paradox is a contradiction, the solution of which provides a deeper insight, see Brockhaus (1998). The above contradiction is called the *space paradox*. It is solved next:

6.3 Solution of the space paradox

In this section, a solution of the space paradox is derived, for the case of natural homogeneous space.

The space paradox has five premises: There are four founded premises about space and its volume V, see section (6.1), parts (1) - (4), part (5) is not used here: isotropy, the positive dark energy density, the energy speed relation of SRT (which is correct in the used ACS), and the zero rest energy E_0. And there is one hardly founded premise: the concept of space as a single entity. Therefore, space is not a single entity.

As space is not a single object, it must consist of many parts of the volume V. These parts δV are analyzed next. Thereby, a part of the space with its volume V is called a *volume portion (VP)*.

Hereby, parts of volume with at least one local maximum of volume are analyzed. Thereby, for each part, one such maximum is used in order to localize that part δV. Such a part is called a *localized VP*.

Since the energy and volume of space have the speed $v = c$, the above parts δV must have the same speed. For instance, each part δV_j has its speed

$$v_j = c. \tag{47}$$

In general, a part of volume is called *volume portion*.

6.4 Isotropy formation

The isotropy forms as follows: Since the Big Bang, the space expands. This is caused by the permanent formation of indivisible volume portions VP_j, see Carmesin (2021b, 2025e). Each such VP has a random velocity $\vec{v}_j$ with the speed c. The sum of the velocities of N VPs represents a random walk. This should be isotropic. The process of the formation of isotropy as a function of N is investigated in a computer simulation: For N such velocity vectors $\vec{v}_j$, the averaged velocity components are evaluated, $\bar{v}_{k,N}$, with $k = 1$, $k = 2$ or $k = 3$. The squared differences $s_{3,N} = (\bar{v}_{1,N} - \bar{v}_{2,N})^2$, $s_{2,N} = (\bar{v}_{1,N} - \bar{v}_{3,N})^2$, and $s_{1,N} = (\bar{v}_{2,N} - \bar{v}_{3,N})^2$ are indicators for anisotropy. Accordingly, the root of the average is a combined indicator for anisotropy: $\sigma := \sqrt{\frac{s_{1,N}+s_{2,N}+s_{3,N}}{3}}$.

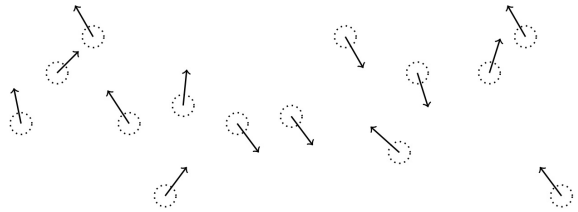

Figure 7: Volume portions δV_j with speed $v_j = c$ (dotted) of homogeneous space with different normalized direction vectors $\vec{e}_j$ of the velocity $\vec{v}_j = c \cdot \vec{e}_j$. The average of the velocities $\vec{v}_j$ is zero. This causes global isotropy of space consisting of rapidly moving volume portions. As a consequence, this solves the space paradox, see Fig. (8).

In an isotropic set of velocities, the combined indicator σ decreases proportional to $1/\sqrt{N}$, in the average. This has been investigated with a respective computer experiment, see Fig. (8).

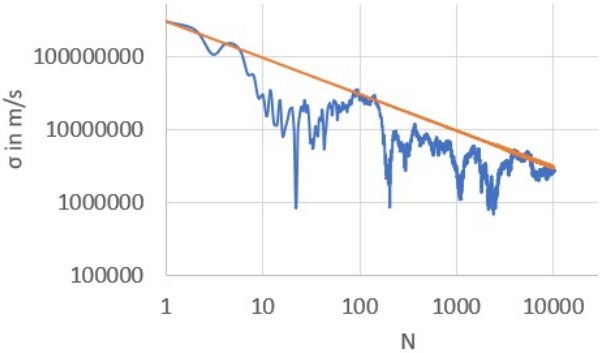

Figure 8: The combined indicator for anisotropy: σ is shown as a function of the number of vectors N (blue). As expected in an isotropic set of vectors, this indicator decreases proportional to $1/\sqrt{N}$, in the average. This shows how space, which is a stochastic average of indivisible volume portions, becomes increasingly isotropic, when the number N of indivisible VPs increases.

6.5 Indivisible volume portions

Next, for the case of a homogeneous universe and space, and for the case of a usual density ρ_{hom}, The following question is analyzed:

Can such a part δV_j with $v_j = c$ consist of smaller parts δV_k?

Hereby, a usual density ρ_{hom} is a density below an ultrahigh critical density $\rho_{cr.,\ space-symmetry-breaking}$ at which the symmetry of space breaks in a phase transition. This can occur in a phase transition from space to matter in the Higgs (1964) mechanism. Moreover, this can take place in a dimensional phase transition, see Carmesin (2017, 2019, 2021b,a)).

If such a part δV_j of space, with $v_j = c$, would consist of smaller parts δV_k, then the following would be implied:

(2.1) Each smaller part δV_k would have the speed $v_k = c$, as the energy and volume of space have the speed $v = c$.

(2.2) Consequently, each part δV_k would have a velocity $\vec{v}_k = c \cdot \vec{e}_k$, with a direction vector $\vec{e}_k$ with norm one.

(2.3) As the considered universe is homogeneous (see part (2)), there is no source that could provide a uniform direction of the direction vectors $\vec{e}_k$.

(2.4) Hence, the velocity $\vec{v}_j$ of the considered part δV_j with $v_j = c$ would be an average of the velocities $\vec{v}_k$. Thereby, as a consequence of the different direction vectors $\vec{e}_k$ in part (2.3), the velocity $\vec{v}_j$ would have an absolute value smaller than c, i. e. $|\vec{v}_j| = v_j < c$. This would contradict the speed $v_j = c$ in Eq. (47).

(2.5) Therefore, the parts δV_j with speeds $v_j = c$ cannot consist of smaller parts. This is the answer to the question in (2). This implies that the parts δV_j with $v_j = c$ are indivisible. Such a part δV_j with its speed $v_j = c$ is called *indivisible volume portion*, indivisible VP.

(3) Next, it is shown how the indivisible VPs solve the space paradox:

(3.1) The energy and volume of space have the speed c, and the energy of space obeys $E^2 \cdot \left(1 - \frac{v^2}{c^2}\right) = E_0^2 = 0$, as space consists of indivisible VPs δV_j with the speed $v_j = c$.

(3.2) Moreover, the velocities $\vec{v}_j = c \cdot \vec{e}_j$ of the indivisible VPs have stochastic direction vectors $\vec{e}_j$, that are distributed isotropically. Hence, these velocities average to zero.

(3.3) As a consequence, space is isotropic at a universal scale, see Fig. (7). In this manner, the space paradox is solved.

Therefore, we obtain the following deep insight, the *stochastic property of space*:

IN A HOMOGENEOUS AND ISOTROPIC UNIVERSE, SPACE IS A STOCHASTIC AVERAGE OF MANY INDIVISIBLE VOLUME PORTIONS δV_j, EACH WITH THE SPEED $v_j = c$. Hereby, the velocities $\vec{v}_j$ of the volume portions average to zero.

(4) The solution has been generalized to heterogeneous space: The early universe was very homogeneous and isotropic, see Planck-Collaboration (2020). The heterogeneity of the mass distribution in the universe increased gradually, and thereby the heterogeneity of space evolved gradually, see e. g. Peebles and Bharat (1988), Mandal and Nadkarni-Ghosh (2020), Carmesin (2018, 2021b, 2025e). Therefore, the natural heterogeneous space is a slight variation of the natural homogeneous and isotropic space. Details of that slight variation are presented in Carmesin (2024a, 2025e).

6.6 Each indivisible VP exists within an underlying VP

In this section, a very valuable and insightful description of VPs is developed. With it, a very general differential equation (DEQ) of the dynamics of VPs is derived in the following section.

Here and in the following, mathematically, a VP could be arbitrarily small. Physically, an indivisible VP has a kind of quantization. Accordingly, the size is limited from below. In particular, a corresponding Heisenberg (1927) uncertainty relation limits the standard deviation of an indivisible VP from below.

Additional volume: In this section, an indivisible VP δV_j is analyzed within the underlying volume portion, in which it exists. There are two ways to describe this: Firstly, δV_j is part of the underlying volume portion, in which δV_j exists. This underlying volume portion is called ΔV_L. Secondly, δV_j is an additional part of the remaining volume. This remaining volume is called δV_R. Its amount is as follows:

$$\Delta V_R = \Delta V_L - \delta V_j \tag{48}$$

Consequently, δV_j is an *additional volume* that is combined with ΔV_R. More generally, the indivisible VP δV_j can be generalized to each mathematical additional volume δV. In such a case, the above Eq. takes the following form:

$$\Delta V_R = \Delta V_L - \delta V \tag{49}$$

In order to derive general laws of physics, this additional volume δV is normalized in the next section:

Relative additional volume: In general, in order to derive general laws of physics, it is valuable to use intensive quantities rather than extensive quantities, see Redlich (1970). In the present case of a VP, it is useful to utilize the ratio of its additional volume δV and its complete or enlarged volume δV_L. Such ratios are formed and analyzed in detail in this section:

That ratio is called *relative additional volume* ε_L:

$$\varepsilon_L := \frac{\delta V}{\Delta V_L}. \tag{50}$$

EACH VP HAS A CORRESPONDING RELATIVE ADDITIONAL VOLUME ε_L.

Examples of parts of space: In this paragraph, essential parts of natural space with the volume V are analyzed.

(1) Additional volume in the vicinity of a mass M:

In the vicinity of a mass M, there occurs additional volume δV. It is at rest relative to M. Moreover, in the vicinity of M, the ACS is nearly at rest at M, see Carmesin (2025e), Carmesin (2025d), Carmesin (2025c). Consequently, the speed of the additional volume in the vicinity of a mass is clearly smaller than c, i. e. $v < c$. Each additional volume with a speed $v < c$ must be a stochastic average of the indivisible VPs δV_j with their speeds $v_j = c$, as space with its volume V consists of indivisible VPs δV_j with their speeds $v_j = c$. This is the case for homogeneous and isotropic space and for the case of heterogeneous space which is a slight variation of homogeneous and isotropic space.

Altogether, additional volume that is at rest in the vicinity of a mass M is a stochastic average of indivisible VPs.

(2) Relative additional volume ε_L:

In general, a VP δV is located within an underlying VP ΔV_L. The relative additional volume ε_L is the following ratio of the VP δV and of its underlying VP ΔV_L:

$$\varepsilon_L := \frac{\delta V}{\Delta V_L} = \frac{\Delta L \cdot \Delta x \cdot \Delta y - \Delta R \cdot \Delta x \cdot \Delta y}{\Delta L \cdot \Delta x \cdot \Delta y}$$
$$= \frac{\Delta L - \Delta R}{\Delta L} = \frac{\delta L}{\Delta L}, \quad \text{with } \delta L := \Delta L - \Delta R. \tag{51}$$

Thereby, the ratio $\frac{\delta L}{\Delta L}$ is usually interpreted as a tensor element, whereby the L - direction is the z - direction or the 3 - direction, for instance:

$$\varepsilon_{zz} := \frac{\delta z}{\Delta z} = \varepsilon_{jj}, \quad \text{with } j = 3. \tag{52}$$

In general, a volume portion VP δV represents a change of an underlying VP ΔV_L, and this change represents a tensor element or tensor. Thereby, typically, the change of each VP ΔV has a quadrupolar structure. A dipolar structure is excluded, as volume cannot be negative. Therefore, each change of an underlying VP ΔV can be described by a tensor of rank two. It is called *change tensor* ε_{ij}, see Carmesin (2021b, 2025e). In general, an element ε_{ij} of a change tensor is the ratio of the change δL_i divided by the underlying length ΔL_j:

$$\varepsilon_{ij} := \frac{\delta L_i}{\Delta L_j}. \tag{53}$$

Hereby, for each normalized direction vector $\vec{e}_j$, the underlying length ΔL_j is the sum of the original length ΔR_j and the change δL_j:

$$\Delta L_j := \Delta R_j + \delta L_j. \tag{54}$$

In general, indivisible VPs can have the structure of a change tensor as well, see Fig. (9).

(3) Gravitational wave:

Without loss of generality, a gravitational wave can be described as follows, see e. g. Landau and Lifschitz (1971): It has an angular frequency ω. At a location, a gravitational wave has one direction of propagation $\vec{e}_z$, and two transverse directions $\vec{e}_x$ and $\vec{e}_y$. There are two possible modes. In a first mode, the elongations are $\varepsilon_{xx} \cdot \cos(\omega t)$ and $\varepsilon_{yy} \cdot \cos(\omega t)$, with $\varepsilon_{xx} = \varepsilon_{yy}$, see Fig. (9). The second mode is equal to the first mode rotated by 45^o around $\vec{e}_z$.

The elongations and the velocity of the gravitational wave can be measured with help of a Michelson interferometer. For instance, Abbott (2016) measured the amplitude $\varepsilon_{xx,max} = 1 \cdot 10^{-21}$.

In the theory of waves, the above observed gravitational wave is a wave with a coherence length that amounts several wave lengths. Accordingly, a gravitational wave could be interpreted as a coherent state in the framework of quantum physics, if quantum physics is applicable.

6.7 Dynamics of volume portions

In this section, the dynamics of an arbitrary VP is described by its relative additional volume. The result is achieved with help of calculus or standard analysis only. As a consequence, the dynamics of VPs derived here is very general.

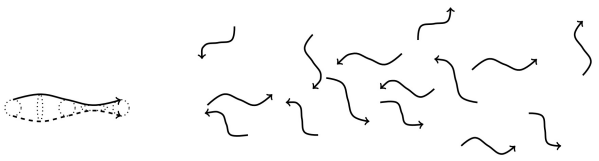

Figure 9: Volume portions (VPs) δV_j with speed $v_j = c$ with different velocities $\vec{v}_j = c \cdot \vec{e}_j$: In general, each VP can include a change as marked at the left. In principle, each VP δV_j can be characterized very precisely by that change. For instance, the change of a VP δV_j moves with its velocity $\vec{v}_j$, and typically, it has a quadrupolar structure. A dipolar structure is excluded, as volume cannot be negative. At the right, these changes are indicated by wiggly lines, for simplicity. The average of the velocities $\vec{v}_j = c \cdot \vec{e}_j$ is zero. This causes global isotropy of space consisting of volume portions with speeds $v_j = c$. Therefore, this solves the space paradox.

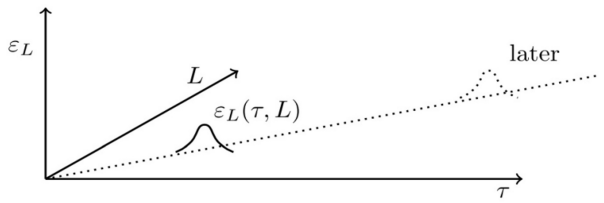

Figure 10: A VP with a relative additional volume $\varepsilon_L(\tau, L)$ with a local maximum is shown as a function of location L and time τ. Thereby, the location L summarizes the three-dimensional vector $\vec{L}$ in such a manner, that the length of the path of the VP is described by L.

Firstly, the applicability of calculus or standard analysis is investigated:

Calculus or analysis are a mathematical tool, such as algebra and stochastics. Thereby, calculus or analysis do not include a prejudice about the continuity of space and time. The reason is that in the present investigation, space is a stochastic average of VPs. Hereby, VPs will be characterized by eigenvalues with a spectrum of eigenvalues. This spectrum can turn out to be discrete, continuous or partially discrete and partially continuous. As calculus or analysis are used in this study, these fields of mathematics do not necessarily include a prejudice about the discreteness or continuity of space.

In contrast, an exclusion of calculus and analysis would include a prejudice about the discreteness or continuity of space.

In fact, the space paradox and the implied structure of space as a stochastic average of VPs does already deduce an essential degree of discreteness of space. And it is important to investigate the amount of discreteness and continuity of these VPs in the following.

Secondly, the differential equation, DEQ, of VPs is derived:

We consider VPs that can be localized by their form. Accordingly, each localized VP has a local maximum of its relative additional volume ε_L. It is a function of its three-dimensional position vector $\vec{L}$ and of the time τ. It is illustrated in Fig. (10), whereby the three-dimensional position vector is summarized by a position L. Altogether, a localized VP can be described by a function $\varepsilon_L(\tau, \vec{L})$ with a local maximum. If there should be several local maxima or a set of local maxima, then one local maximum can be chosen as a convention.

As a fact of calculus or of analysis, at the local maximum, the change of $\varepsilon_L(\tau, \vec{L})$ is zero. Thus, the total derivative is zero:

$$d\varepsilon_L(\tau, \vec{L}(\tau)) = 0 \tag{55}$$

That derivative is evaluated with help of partial derivatives:

$$d\varepsilon_L(\tau, \vec{L}(\tau)) = \frac{\partial}{\partial \tau}\varepsilon_L(\tau, \vec{L})d\tau + \frac{\partial}{\partial \vec{L}}\varepsilon_L(\tau, \vec{L})d\vec{L} = 0. \tag{56}$$

The VP moves parallel to a corresponding direction unit vector $\vec{e}_v$ of its velocity $\vec{v} = \frac{\partial \vec{L}}{\partial \tau}$. Therefore, during a time $d\tau$, the vector $\vec{L}$ changes by the amount $d\vec{L}$ = $v \cdot d\tau \cdot \vec{e}_v$. With it, the total derivative in Eq. (56) is

$$\frac{\partial}{\partial \tau}\varepsilon_L(\tau, \vec{L})d\tau + v \cdot \vec{e}_v \cdot \frac{\partial}{\partial \vec{L}}\varepsilon_L(\tau, \vec{L})d\tau = 0. \tag{57}$$

The above Eq. is divided by $d\tau$. Moreover, the Eq. is solved for $\frac{\partial}{\partial \tau}\varepsilon_L$:

$$\frac{\partial}{\partial \tau}\varepsilon_L(\tau, \vec{L}) = -v \cdot \vec{e}_v \cdot \frac{\partial}{\partial \vec{L}}\varepsilon_L(\tau, \vec{L}), \quad \text{each indivisible VP has} \quad v = c \tag{58}$$

This is the differential equation, DEQ, of VPs or of *volume dynamics (VD)*. A Lorentz invariant form of the DEQ is achieved as follows. The square is applied to Eq. (58), and the right hand side is subtracted,

$$\left(\frac{\partial \varepsilon_L}{\partial \tau}\right)^2 - v^2 \cdot \left(\frac{\partial \varepsilon_L}{\partial \vec{L}}\right)^2 = 0, \quad \text{each indivisible VP has} \quad v = c \tag{59}$$

EACH LOCALIZED VP FULFILLS THE VOLUME DYNAMICS in Eq. (58) or in the Lorentz invariant Eq. (59).

For the following reasons, the derived dynamics is very founded and insightful: The derived DEQ of VD describes the dynamics of a VP with at least one local maximum. The derivation uses no postulate or unfounded hypothesis. In contrast, general relativity uses postulates such as the Einstein Hilbert action or the Einstein field equation, see Einstein (1915), Hilbert (1915). Similarly, quantum physics uses 'guessed' postulates, see e. g. Hilbert et al. (1928), Sakurai and Napolitano (1994), Ballentine (1998). Also gravity uses 'guessed' postulates or restrictions. Examples are the restriction to physics without quanta in general relativity, see Einstein (1915), and in Newton's gravity, see Newton (1687). Another example is the graviton hypothesis. Thereby, gravity uses hypothetic quanta, see e. g. Blokhintsev and Galperin (1934).

Indeed, we will show later that the DEQ of VD implies gravity and curvature of space and time. Moreover, we will show that the DEQ of VD implies the postulates of quantum physics. In particular, based on the VD, we derive the Schrödinger equation in the next section.

6.8 Discussion of the VD

The differential Eq. of VD is a linear differential equation for the relative additional volume ε_L. As a consequence, its solutions are numerically stable, as chaotic behaviour is caused by a nonlinear dynamics only, see Wiggins (2003).

In fact, relative additional volume ε_L describes the volume portions at a classical level. But the volume dynamics includes even more dynamical behaviour. For it, a time derivative will be applied to the differential Eq. of VD. As a consequence, the resulting differential Eq. will describe wave functions Ψ, which describe indivisible volume portions. In general, these wave functions can even be complex, and their properties imply the postulates of quantum physics.

In this manner, the transition from a classical stochastic description of indivisible volume portions to a description with complex-valued wave functions and quantum postulates is derived in the present paper. This will be derived in the following sections (6.9, 7 and 8).

These postulates imply phenomena such as nonlocality, see Aspect et al. (1982), Zeilinger et al. (1988), Clauser and Horne (1974) or teleportation, see Ma et al. (2012). Thereby, the postulates derived for volume portions can be applied to matter, as matter emerges from vacuum or volume by a phase transition, see Higgs (1964), Carmesin (2021a, 2022c).

6.9 Derivation of the Schrödinger equation

In this section, we show that each VP fulfills a *generalized Schrödinger equation (GSEQ)*, which implies the usual *Schrödinger equation (SEQ)*, which holds for the special case of a non-relativistic mass M.

The volume dynamics implies the GSEQ: In this section it is shown, that VPs with their VD imply the GSEQ.

(1) In a first investigation, the geometry of relative additional volume is analyzed:

For each VP, the DEQ (58) of VD is fulfilled. Thereby, the VP moves in the direction $\vec{e}_v$ of its velocity, see Fig. (10).

In general, a relative additional volume with an increase δL_3 with the normalized direction vector $\vec{e}_3$ and with a propagation of indivisible VPs in the same direction, and with an underlying length ΔL_3, is called *unidirectional* relative additional volume $\varepsilon_{L,33}$, see Eqs. (52, 53 and 54). For more information about such tensors see e. g. Landau and Lifschitz (1971), Lee (1997), Carmesin (2021b, 2024a, 2025e).

(2) Next, each VP is described by the DEQ of VD. In that DEQ, $v = c$ is inserted. Additionally, the time derivative is applied, so that the relative additional volume $\varepsilon_{L,jj}$ becomes $\frac{\partial}{\partial\tau}\varepsilon_{L,jj}$, which is usually expressed by $\dot{\varepsilon}_{L,jj}$. As a consequence, the DEQ of VD implies the following DEQ:

$$\frac{\partial}{\partial\tau}\dot{\varepsilon}_{L,jj} = -c\cdot\vec{e}_v\cdot\frac{\partial}{\partial\vec{L}}\dot{\varepsilon}_{L,jj} \qquad (60)$$

(3) Next, as an equivalence transformation of the above DEQ, the factor $i\hbar$ is multiplied. This multiplication is also physically equivalent, as the system of units can be chosen freely. And the factor $\hbar$ is one in natural units, see Tipler and Llewellyn (2008), pages 673-674. Consequently, the DEQ of VD implies the following DEQ:

$$i\hbar\cdot\frac{\partial}{\partial\tau}\dot{\varepsilon}_{L,jj} = c\cdot\vec{e}_v\cdot\left[-i\hbar\cdot\frac{\partial}{\partial\vec{L}}\right]\dot{\varepsilon}_{L,jj} \qquad (61)$$

Moreover, for the case of an indivisible VP, this indivisibility corresponds to the quantum property with its universal unit of quantization, the Planck (1900) constant h or its reduced version $\hbar := \frac{h}{2\pi}$.

Accordingly, the correspondence principle is applicable, see Tipler and Llewellyn (2008) page 160.

Consequently, the rectangular bracket is identified with the momentum operator, see (Carmesin, 2024a, chapter 9):

$$i\hbar \cdot \frac{\partial}{\partial \tau} \dot{\varepsilon}_{L,jj} = \vec{e}_v \cdot c \cdot \hat{\vec{p}} \cdot \dot{\varepsilon}_{L,jj} \tag{62}$$

In this DEQ, $\dot{\varepsilon}_{L,jj}$ represents a rate. That rate is normalized by a factor t_n. In physics, t_n has the dimension time and the unit second. Consequently, the normalized rate $t_n \cdot \dot{\varepsilon}_{L,jj}$ is dimensionless and has the unit one. It will be shown that the normalized rate has the role of a wave function in the above DEQ. Accordingly, the normalized rate is called wave function Ψ. Of course, this can be regarded as an abbreviation, if desired. As a consequence, the DEQ of VD implies the following DEQ:

$$i\hbar \cdot \frac{\partial}{\partial \tau} \Psi = c \cdot \vec{e}_v \cdot \hat{\vec{p}} \cdot \Psi \tag{63}$$

$$\Psi := t_n \cdot \dot{\varepsilon}_{L,jj} \tag{64}$$

The product of the momentum operator and the direction vector of propagation, $\vec{e}_v \cdot \hat{\vec{p}}$, is the operator of the absolute value of the momentum $\hat{p}$:

$$i\hbar \cdot \frac{\partial}{\partial \tau} \Psi = c \cdot \hat{p} \cdot \Psi \tag{65}$$

In the present case of a VP that propagates with the speed c, special relativity implies that the product of c and the momentum p is the energy E. Consequently, according to the correspondence principle, see Tipler and Llewellyn (2008), pages 673-674, the product of c and the momentum operator is the energy operator:

$$i\hbar \cdot \frac{\partial}{\partial \tau} \Psi = \hat{E} \cdot \Psi \tag{66}$$

This Eq. has the form of a Schrödinger equation, SEQ. However, the SEQ holds for non-relativistic objects. In contrast, this DEQ holds for relativistic objects too, and it implies the SEQ for non-relativistic objects, see next paragraph. Thus, this DEQ is the GSEQ.

EACH VP FULFILLS THE GSEQ (66) AND HAS A PHYSICALLY REAL WAVE FUNCTION $\Psi \propto \dot{\varepsilon}_{L,rr}$ in Eq. (64). Thereby, according to the Hacking (1983) criterion, a wave function has an extraordinary physical reality, as it can be manipulated even in a nonlocal manner, see e. g. Aspect et al. (1982).

The volume dynamics implies the SEQ: In this section it is shown, that VPs with their VD imply the SEQ.

For each localizable quantum object at $v \leq c$, the following is implied:

(1) For the case of **ultrafast objects**, with $p^2c^2 \gg m_0^2c^4$, see e. g. (Workman, 2022, Eq. 14.38), an energy eigenvalue is obtained by the following linear approximation of the energy momentum relation $E = \sqrt{p^2c^2 + m_0^2c^4}$ with respect to the small ratio $\frac{m_0^2c^4}{p^2 \cdot c^2}$:

$$E \doteq p \cdot c + \frac{m_0^2c^4}{2 \cdot p \cdot c} \tag{67}$$

Hereby, $\doteq$ marks the first order approximation for small $\frac{m_0^2c^4}{p^2 \cdot c^2}$. The corresponding linear approximation of the GSEQ is obtained by replacing the eigenvalue p by its operator $\hat{p}$:

$$i\hbar \frac{\partial}{\partial \tau} \Psi \doteq \left(\hat{p} \cdot c + \frac{m_0^2c^4}{2 \cdot \hat{p} \cdot c} \right) \cdot \Psi \tag{68}$$

(2) For the case of **slow objects**, with $p^2c^2 \ll m_0^2c^4 =: E_0^2$, the following holds:

(2a) An energy eigenvalue of the energy is obtained by the following linear approximation of the energy momentum relation $E = \sqrt{p^2c^2 + m_0^2c^4}$ with respect to the small ratio $\frac{p^2 \cdot c^2}{E_0^2}$:

$$E \doteq E_0 + \frac{p^2}{2 \cdot m_0} \tag{69}$$

(2b) The corresponding linear approximation of the GSEQ is obtained by replacing the eigenvalue p by its operator $\hat{p}$.

$$i\hbar \frac{\partial}{\partial \tau} \Psi_{E_0} \doteq \left(E_0 + \frac{\hat{p}^2}{2 \cdot m_0} \right) \cdot \Psi_{E_0} \tag{70}$$

Hereby, the wave function includes the rest energy E_0. Accordingly, the wave function is named Ψ_{E_0}. In general, the following squares are equal:

$$\hat{p}^2 = \hat{\vec{p}}^{\ 2} \tag{71}$$

(2c) The wave function is factorized:

$$\Psi_{E_0} = \Psi \cdot \exp\left(\frac{E_0 \tau}{i\hbar} \right) \tag{72}$$

The left hand side of Eq. (70) is evaluated with the product rule:

$$E_0 \Psi_{E_0} + \exp\left(\frac{E_0 \tau}{i\hbar} \right) i\hbar \frac{\partial \Psi}{\partial \tau} \doteq \left(E_0 + \frac{\hat{p}^2}{2m_0} \right) \cdot \Psi_{E_0} \tag{73}$$

(2d) In the above DEQ, $E_0\Psi_{E_0}$ is subtracted. The resulting DEQ is divided by $\exp\left(\frac{E_0\tau}{i\hbar}\right)$. As a consequence, the SEQ proposed or postulated by Schrödinger (1926) is derived from the VD:

$$i\hbar\frac{\partial}{\partial\tau}\Psi\doteq\frac{\hat{p}^2}{2\cdot m_0}\cdot\Psi=\hat{H}\Psi \tag{74}$$

Additionally, $\hat{H}$ can include a potential energy:

$$i\hbar\frac{\partial}{\partial\tau}\Psi\doteq\frac{\hat{p}^2}{2\cdot m_0}\Psi+E_{pot}\Psi=\hat{H}\Psi \tag{75}$$

Interpretation of VPs and masses: In this section, the relation between VPs and masses is elaborated on the basis of the above dynamics of the VD, the GSEQ and the SEQ, and of the Higgs (1964) mechanism:

Some elementary particles form their mass by a phase transition, see Higgs (1964), Aad (2012), Chatrchyan (2012), Navas et al. (2024), Carmesin (2021b), Carmesin (2021a), Carmesin (2022c): In physics, see Guericke (1672), Casimir (1948), Tipler and Llewellyn (2008), empty space is called *vacuum*, and its energy density is the density u_{DE} of dark energy, see Perlmutter et al. (1998), Huterer and Turner (1999).

As shown by the space paradox, the vacuum is a stochastic average of indivisible VPs. As a consequence, the above phase transition transforms indivisible volume portions to a mass.

In a typical phase transition, objects change from one phase to another phase. Thereby, these objects are described by the same fundamental dynamics in the first phase, in the second phase and during the transition. An example is the phase transition of condensation, see van der Waals (1873), Landau and Lifschitz (1980).

In the present case, such a fundamental dynamics that holds in the first phase, in the second phase and during the transition has been derived. It is the DEQ of VD. It holds for VPs in the first phase, and it implies the SEQ that holds for the masses in the second phase. A description of the phase transition in the framework of the VPs is elaborated in Carmesin (2022c).

Of course, the question remains how a mass can emit its wave function. This will be derived in the next section: In part (7), it is shown that the VPs provide gravity as well as the local curvature of space and time as a byproduct. It has already been shown that a mass causes additional volume and VPs, see corresponding paragraphs.

EACH MASS M FULFILLS THE SEQ (75) IMPLIED BY THE GSEQ. M can be formed from VPs via a phase transition, see Higgs (1964), Carmesin (2021a, 2022c).

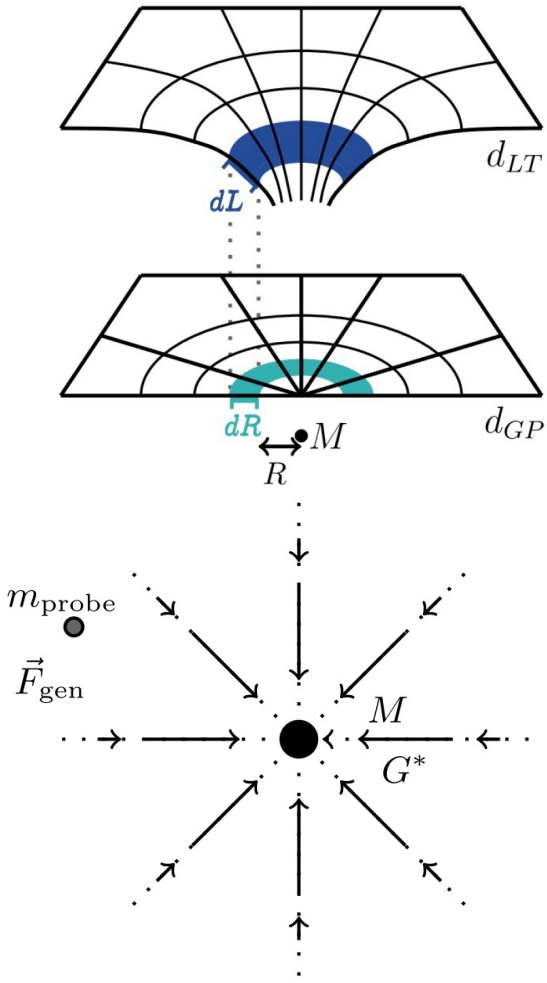

Figure 11: In the vicinity of a field generating mass M, the space is curved (upper map), and in the limit $M\to 0$, the space is flat (lower map), see Fig (6). The physical situation is expressed with help of a field in the lower part.

7 Emergent gravity and curvature

In the vicinity of a mass M, there occurs a curvature of space, as well as an exact gravitational potential and field, see Fig. (6). Next it is shown how these phenomena are implied by the DEQ of VD:

7.1 Potential and field

In this section, an exact generalized potential and generalized field are derived from the volume portions.

Generalized potential and field: In the vicinity of a mass M, see Fig. (11), the unidirectional radial relative additional volume $\varepsilon_{L,rr}$ exhibits the following properties. Hereby, spherical polar coordinates (r, ϑ, φ) with M at the origin, dR at $M \to 0$ and dL at $M \neq 0$ in Fig. (11) are used:

(1) For each indivisible VP δV_j, the relative additional volume $\varepsilon_{L,rr,j}(\tau, \vec{L})$ propagates according to the DEQ of VD.

(1.1) That DEQ is multiplied by c:

$$c \cdot \frac{\partial}{\partial \tau} \varepsilon_{L,rr,j}(\tau, \vec{L}) = \vec{e}_v \cdot \frac{\partial}{\partial \vec{L}} \left(-c^2 \cdot \varepsilon_{L,rr,j}(\tau, \vec{L}) \right) \tag{76}$$

(1.2) At an event $(\tau, \vec{L})$, including the set $\mathcal{S}$ of its surrounding events in a time interval $\tau_i \in [\tau - \Delta\tau, \tau + \Delta\tau]$ and in a ball $|\vec{L}_i - \vec{L}| \leq \Delta L$, with $\vec{L}$ in the vicinity of the mass, the sum of the relative additional volume of all indivisible VPs δV_j is applied:

$$c \cdot \frac{\partial}{\partial \tau} \sum_{j \ in \ \mathcal{S}} \varepsilon_{L,rr,j}(\tau, \vec{L}) = \vec{e}_v \cdot \frac{\partial}{\partial \vec{L}} \left(-c^2 \cdot \sum_{j \ in \ \mathcal{S}} \varepsilon_{L,rr,j}(\tau, \vec{L}) \right) \tag{77}$$

(1.3) The bracket in the above DEQ has the form of a generalized potential $\Phi_{gen}(\tau, \vec{L})$

$$\Phi_{gen}(\tau, \vec{L}) := -c^2 \cdot \sum_{j \ in \ \mathcal{S}} \varepsilon_{L,rr,j} \tag{78}$$

Hereby, the potential is generalized, as it describes volume portions, since $\varepsilon_{L,rr,j}$ is the relative additional volume of an indivisible VP.

(1.4) The negative gradient of that generalized potential is the generalized field $\vec{G}_{gen}$, see Fig. (11):

$$\vec{G}_{gen}(\tau, \vec{L}) := -\frac{\partial}{\partial \vec{L}} \left(-c^2 \cdot \sum_{j \ in \ \mathcal{S}} \varepsilon_{L,rr,j} \right) = -\frac{\partial}{\partial \vec{L}} \Phi_{gen}(\tau, \vec{L}) \tag{79}$$

The generalized field $\vec{G}_{gen}$ is the exact gravitational field $\vec{G}^*_{exact}$, see section (7.3). Moreover, the field is a sum of the following indivisible *field parts* $\vec{G}_j$ of the indivisible volume portions $\varepsilon_{L,rr,j}$:

$$\vec{G}_{gen}(\tau, \vec{L}) := \sum_{j \ in \ \mathcal{S}} \vec{G}_j(\tau, \vec{L}) = \vec{G}^*_{exact}(\tau, \vec{L})$$

$$\text{with} \quad \vec{G}_j(\tau, \vec{L}) := c^2 \frac{\partial}{\partial \vec{L}} \varepsilon_{L,rr,j} \tag{80}$$

(1.5) Therefore, the DEQ of VD in Eq. (76) takes the form of the following *rate gravity relation*:

$$c \cdot \frac{\partial}{\partial \tau} \sum_{j \ in \ \mathcal{S}} \varepsilon_{L,rr,j} = \vec{e}_v \cdot \frac{\partial}{\partial \vec{L}} \Phi_{gen}(\tau, \vec{L}) = -\vec{e}_v \vec{G}_{gen}(\tau, \vec{L}) \tag{81}$$

The potential and field in the above equation are generalized to the respective quantities for one indivisible VP δV_j. Thereby, the potential is

$$\Phi_{gen,j}(\tau, \vec{L}) = -c^2 \varepsilon_{L,rr,j}(\tau, \vec{L}), \tag{82}$$

and the field is as follows:

$$\vec{G}_{gen,j}(\tau, \vec{L}) = -\frac{\partial}{\partial \vec{L}} \Phi_{gen,j}(\tau, \vec{L}) = c^2 \frac{\partial}{\partial \vec{L}} \varepsilon_{L,rr,j}. \tag{83}$$

These relations are results of the VD. Formally, these results can be obtained by an application of the above average with one indivisible VP only.

For comparison, expectation values of the field have been derived from the VD as follows: Firstly, a quantum field theory has been derived from the VD. Secondly, the expectation value of a field has been derived from the quantum field theory, see Carmesin (2024a, 2025e).

(2) For these indivisible VPs, and for each event $(\tau, \vec{L})$, that rate gravity relation can be expressed with help of the following *rate gravity scalar* RGS_{gen}:

$$RGS_{gen} := \left(c \cdot \frac{\partial}{\partial \tau} \sum_{j \ in \ \mathcal{S}} \varepsilon_{L,rr,j} \right)^2 - \vec{G}^2_{gen}, \quad \text{thus} \tag{84}$$

$$RGS_{gen} = \left(c \cdot \frac{\partial}{\partial \tau} \sum_{j \ in \ \mathcal{S}} \varepsilon_{L,rr,j} \right)^2 - \sum_{k=1}^{D} G^2_{gen,k} \quad \text{and} \tag{85}$$

$$RGS_{gen} = \left(c \cdot \frac{\partial}{\partial \tau} \sum_{j \ in \ \mathcal{S}} \varepsilon_{L,rr,j} \right)^2 - \left(c \frac{\partial}{\partial \vec{L}} \Phi_{gen} \right)^2 \tag{86}$$

$$\text{and} \quad RGS_{gen} = 0 \tag{87}$$

Hereby, the dimension of space is marked by D.

(3) For each underlying volume ΔV, and for each event $(\tau, \vec{L})$, with a gravitational parallax distance R from M, the generalized field is proportional to $\frac{1}{R^2}$:

$$|\vec{G}_{gen}| \propto \frac{1}{R^2}, \quad \text{for } D=3, \quad \text{and for } \Delta V \tag{88}$$

This result is derived as follows:

(3.1) Eq. (81) is multiplied by $\vec{e}_v$. Hence, the field is as follows:

$$\vec{e}_v \cdot c \cdot \frac{\partial}{\partial \tau} \sum_{j \ in \ \mathcal{S}} \varepsilon_{L,rr,j} = -\vec{G}_{gen}(\tau, \vec{L}) \tag{89}$$

(3.2) Integration with respect to τ from zero to a time $\delta\tau$ yields:

$$\vec{e}_v \cdot c \cdot \sum_{j \ in \ \mathcal{S}} \varepsilon_{L,rr,j}(\delta\tau) = -\int_0^{\delta\tau} \vec{G}_{gen}(\tau, \vec{L}) d\tau \tag{90}$$

The time $\delta\tau$ is chosen so small that the integral in the above Eq. is approximated by $\delta\tau \cdot \vec{G}_{gen}$. Thus, the field is as follows:

$$\vec{e}_v \cdot c \cdot \sum_{j \ in \ \mathcal{S}} \varepsilon_{L,rr,j}(\delta\tau) = -\delta\tau \cdot \vec{G}_{gen} \tag{91}$$

(3.3) The definition $\varepsilon_{L,rr,j} = \frac{\delta V_{L,rr,j}}{dV_L}$ is used. The energy density u_{vol} of volume is nonzero, as it is approximately the same as u_{DE}, which is nonzero, see Perlmutter et al. (1998), Riess (2000), Smoot (2007). Therefore, the indivisible VP $\delta V_{L,rr,j}$ is proportional to the corresponding energy δE_j. The latter is proportional to the momentum $\delta p_j = \delta E_j / c$, as each VP propagates with the speed c, that is: $\delta V_{L,rr,j} = \frac{\delta E_j}{u_{vol}} = \frac{c \cdot \delta p_j}{u_{vol}}$.

(3.4) The underlying volume dV_L of a shell with center M is considered. It is as follows: $dV_L = A_D \cdot R^{D-1} \cdot dL$. Thus, the field is as follows:

$$-\vec{e}_v \cdot \frac{c^2}{u_{vol} \cdot A_D \cdot dL} \cdot \frac{\sum_{j \ in \ \mathcal{S}} \delta p_j}{\delta\tau} \cdot \frac{1}{R^2} = \vec{G}_{gen} \tag{92}$$

Hereby, the thickness dL of each shell is chosen constant, so that it does not dependent on R. Thence, the first fraction is constant. The 2^{nd} fraction is the momentum current flowing through each shell. It is constant, as no shell causes any momentum. Consequently, $\frac{1}{R^2} \propto |\vec{G}_{gen}|$. q. e. d.

A version of the corresponding result for a dimension $D > 3$ is shown in (Carmesin, 2024a, THM 9).

(4) As M is the source of the field $\vec{G}_{gen}(R)$, that field is proportional to M: $\left|\vec{G}_{gen}(R)\right| \propto \frac{M}{R^2}$.

Thus, there is a universal constant G_{gen} of proportionality:

$$\left|\vec{G}_{gen}(R)\right| = \frac{G_{gen} M}{R^2}, \quad \text{for } D=3. \tag{93}$$

In general, the value of a universal constant, such as G_{gen}, must be obtained from observation. Accordingly, G_{gen} is obtained in the next section. Additionally, the curvature of space is analyzed:

Spin, statistics and the additive structure of VPs, potentials and fields: In general, a VP has the tensor property of a quadrupolar structure. Consequently, it is represented by a tensor of rank two.

Therefore, at the level of quantum physics, an indivisible VP has an integer valued spin, see Landau and Lifschitz (1965), §58, Carmesin (2024d):

$$S = n \cdot \hbar, \quad \text{with a natural number} \quad n. \tag{94}$$

As a consequence, at the level of quantum physics, an indivisible VP is a boson, see Landau and Lifschitz (1965) §64, Carmesin (2024d). Consequently, at the level of quantum physics, an indivisible VP obeys the Bose (1924) statistics, alias Bose - Einstein statistics, see Landau and Lifschitz (1965) §64, Sakurai and Napolitano (1994) section 7.2.

The Bose - Einstein statistics implies that several bosons can exist at the same place. Consequently, the additional volumes $\varepsilon_{L,rr,j}$ caused by different masses m_j can exist simultaneously at each point P in the universe, and these $\varepsilon_{L,rr,j}$ add up at P. This, in turn, implies that the potential $\Phi_{gen}(P)$ at P is the sum of these additional volumes $\varepsilon_{L,rr,j}(P)$ multiplied by $-c^2$. This founds Eq. (78) at the level of quantum physics. As a consequence of this potential, the generalized field $\vec{G}_{gen}(P) = \frac{\partial}{\partial \vec{L}} \Phi_{gen}(P)$ has the same additive structure.

7.2 Curvature in the vicinity of a mass

The DEQ of VD provides the curvature in the vicinity of a mass M as follows:

(1) For the case of a shell with the center M and with the gravitational parallax radius R, the relative additional volume $\varepsilon_{L,rr}$ is as follows:

$$\begin{aligned} \varepsilon_{L,rr} &= \frac{dV_L - dV_R}{dV_L} = 1 - \frac{dV_R}{dV_L} \\ &= 1 - \frac{4\pi R^2 dR}{4\pi R^2 dL} = 1 - \frac{dR}{dL}. \end{aligned} \tag{95}$$

The resulting fraction $\frac{dR}{dL}$ is called *position factor*, see e. g. Carmesin (2024a):

$$\varepsilon_E(R) := \frac{dR}{dL} = 1 - \varepsilon_{L,rr} \tag{96}$$

The fraction $\frac{dL}{dR}$ is identified with the root of the radial tensor element of the metric tensor. It occurs in the vicinity of a mass M.

$$\sqrt{g_{rr}} := \frac{dL}{dR} = \frac{1}{\varepsilon_E(R)}. \tag{97}$$

More generally, at each R, or at each event $(\tau, \vec{L})$ with $|\vec{L}| \geq R$, the curvature can be generalized for the case of a single indivisible VP δV_j, with the relative additional volume $\varepsilon_{L,rr,j}$, as follows:

$$g_{rr,j} := \frac{1}{\varepsilon_{E,j}^2} := \frac{1}{(1-\varepsilon_{L,rr,j})^2}. \tag{98}$$

(2) A DEQ for the position factor is derived: For it, $\frac{\partial}{\partial L}$ is applied to Eq. (96). This implies:

$$\frac{\partial}{\partial L}\varepsilon_E = \frac{\partial R}{\partial L}\frac{\partial}{\partial R}\varepsilon_E = \varepsilon_E \frac{\partial}{\partial R}\varepsilon_E = -\frac{\partial \varepsilon_{L,rr}}{\partial L} \tag{99}$$

The potential $\Phi_{gen} = -c^2\varepsilon_{L,rr}$ is solved for $\varepsilon_{L,rr}$, and this is inserted into Eq. (99):

$$\varepsilon_E(R)\frac{\partial \varepsilon_E}{\partial R} = \frac{\partial \Phi_{gen}/c^2}{\partial L} \tag{100}$$

The gradient $\frac{\partial}{\partial L} = \vec{e}_v \frac{\partial}{\partial \vec{L}}$ is applied:

$$\varepsilon_E(R)\frac{\partial \varepsilon_E}{\partial R} = \vec{e}_v \frac{\partial \Phi_{gen}/c^2}{\partial \vec{L}} \tag{101}$$

The field $-\frac{\partial \Phi_{gen}}{\partial \vec{L}} = \vec{G}_{gen}$ is identified:

$$-\vec{e}_v \frac{1}{c^2}\vec{G}_{gen} = \varepsilon_E(R)\frac{\partial \varepsilon_E}{\partial R} \tag{102}$$

The field and the direction vector are antiparallel. Consequently, the field is as follows:

$$\frac{1}{c^2}|\vec{G}_{gen}| = \varepsilon_E(R)\frac{\partial \varepsilon_E}{\partial R} \tag{103}$$

The field as a function of the mass in Eq. (93) is used:

$$\frac{G_{gen}M}{R^2c^2} = \varepsilon_E(R)\frac{\partial \varepsilon_E}{\partial R} \tag{104}$$

(3) The DEQ for the position factor is solved:

Integration by parts yields:

$$\int \frac{G_{gen}M}{R^2c^2}dR = \int \varepsilon_E(R)d\varepsilon_E \tag{105}$$

The integral is evaluated with a constant K of integration:

$$K - \frac{G_{gen}M}{Rc^2} = \frac{1}{2}\varepsilon_E^2 \tag{106}$$

That result is solved for the position factor:

$$\varepsilon_E = \sqrt{2K - \frac{2G_{gen}M}{c^2}\frac{1}{R}} \tag{107}$$

In the limit $R \to \infty$, there is no curvature. Consequently, $\varepsilon_E = \frac{dR}{dL} = 1$. As a consequence, $2K = 1$. Therefore, the solution of the DEQ provides the position factor as follows:

$$\varepsilon_E = \sqrt{1 - \frac{2G_{gen}M}{c^2}\frac{1}{R}} \tag{108}$$

(4) The position factor in Eq. (108) is compared with observation. For it, the position factor is replaced by the inverse root of the radial tensor element (see Eq. 97):

$$\varepsilon_E = \sqrt{1 - \frac{2G_{gen}M}{c^2}\frac{1}{R}} = \frac{1}{\sqrt{g_{rr}}} \tag{109}$$

Moreover, observation shows that this inverse root of the radial tensor element is as follows, see e. g. Hobson et al. (2006), Stephani (1980):

$$\sqrt{1 - \frac{2GM}{c^2}\frac{1}{R}} = \frac{1}{\sqrt{g_{rr}}} = \sqrt{1 - \frac{R_S}{R}}. \tag{110}$$

Hereby, we use the definition of the Schwarzschild radius $R_S := \frac{2GM}{c^2}$. The comparison of the two relations for the tensor element in Eqs. (109 and 110) shows that the generalized universal constant G_{gen} is the same as Newton's constant of gravitation G. Thus, the generalized field is identified with the exact gravitational field and the generalized potential is identified with the exact gravitational potential. These identified potential and field are exact, as they are derived without any approximation, and as they provide the correct curvature. This exact gravitation, derived here exactly, differs from Newton's law of gravitation, which is an approximation.

IN THE VICINITY OF A MASS, THE INDIVISIBLE VPS CAUSE A GENERALIZED POTENTIAL, A GENERALIZED FIELD, THE GRAVITATIONAL FIELD AND THE CURVATURE OF SPACE AND TIME. The respective Eqs. are derived.

7.3 Discussion of gravity and curvature

In the vicinity of a mass M, the VD provides the relative additional volume $\varepsilon_{L,rr}(r)$ as a function of r. That $\varepsilon_{L,rr}(r)$ provides the exact gravitational potential $\Phi_{exact} = -c^2 \cdot \varepsilon_{L,rr}(r)$. That exact gravitational potential provides the exact gravitational field $\vec{G}^*_{exact} = -\frac{\partial}{\partial \vec{L}} \Phi_{exact}$. In the following, these valuable and insightful properties are analyzed and interpreted:

Transmission of the potential and field: The indivisible VPs δV_j with their relative additional volume $\varepsilon_{L,rr,j}(r)$ provide a net outward propagation. Thereby, these indivisible VPs transmit a nonzero momentum, as the energy density u_{vol} is positive. As a consequence, these indivisible VPs transmit the gravitational interaction. This confirms the idea of the graviton hypothesis proposed by Blokhintsev and Galperin (1934). Moreover, these indivisible VPs explicate the mechanism of the transmission of gravity.

In addition, these indivisible VPs cause and explain the curvature of space. Thereby, the curvature is explained with help of the sum of indivisible VPs. More generally, the curvature of a single indivisible VP has been generalized, see Eqs. (97 and 98).

On the exactness of the potential and field: The generalized potential and field derived here are exact. In contrast, the gravitational potential is only an approximation in Newton's theory. For instance, correction terms depending on the gravitational parallax distance R and on the velocity $\vec{v}$ have been elaborated in Post-Newtonian approximations, see e. g. Yang (2014), Eq. (2.49), Blanchet (2024). Accordingly, the following question arises: How is the exactness achieved here?

Essentially, this is achieved here by the application of especially useful distance measures and coordinates systems:

Firstly, for each point P in the universe, there is an adequate coordinate system (ACS), so that an object at rest in the ACS has the absolute zero of velocity, see Carmesin (2025e,c,d). This ACS is used here. As a consequence, the velocity-terms in Post-Newtonian approximation are zero.

Secondly, two measurable distance measures are used, see Fig. (6): the light travel distance d_{LT}, see e. g. Condon and Mathews (2018), and the gravitational parallax distance d_{GP}, see e. g. Carmesin (2019, 2021b, 2025e), it can also be measured as a circumferential distance, see Moore (2013), (Carmesin, 2023, section 2.6).

Hereby, according to the Hacking (1983) criterion, the light travel distance d_{LT} to a field generating mass M is real according to the Hacking criterion Hacking (1983), as an increase of M can change that distance d_{LT}. In contrast, the gravitational parallax distance d_{GP} to a field generating mass M is idealized, as it represents the limit M to zero of the light travel distance:

$$d_{GP} = \lim_{M \to 0} d_{LT}. \tag{111}$$

This is a typical idealization based on a limit, see Song (2002). Though the gravitational parallax distance d_{GP} is idealized and not real, that distance d_{GP} can be measured, and that distance d_{GP} provides the $\frac{1}{R^2}$ law, see Fig. (11).

Thirdly, the exact potential and field are determined as follows: For the case of a point P, the idealized gravitational parallax distance d_{GP} from P to the field generating mass M is measured or determined by other means. With it, the potential and the field are determined as a function of $d_{GP} = R$, by using the respective equations in this section and paper. The result is exact, as no approximation has been used in the derivation of these equations.

In contrast, in Newton's theory, the flatness of space has been introduced as a postulate. Accordingly, a user might use that postulate and the light travel distance $d_{LT} \neq R$, and the equations for potentials and fields in Newton's mechanics. In such a postulate based determination of the potential or field, the result is an approximation only.

Advantage of the exact potential and field: Altogether, the indivisible VPs cause the transmission of gravity, the exact gravitational potential, the exact gravitational field and the exact curvature of space, in an indivisible and impartible manner. Thereby, by using the adequate coordinate system and the measurable idealized gravitational parallax distance, relatively short, highly structured, and clarifying equations can be used. Moreover, the results are parts of the unification of relativity, gravity and quanta. This unification uses the relative difference $\varepsilon_{L,rr}$, which is based on both distance measures: the real d_{LT} and the idealized d_{GP}.

7.4 Energy density of the gravitational field

In this section, the energy density u_f of a gravitational field $\vec{G}^*$ is introduced and derived.

Measurement of the field's energy density: The energy density of the field can be measured as follows: A rest mass M_{rest} is distributed uniformly in a

shell with a radius R and a small thickness dR, see Fig. (12). That mass is lifted by a radial difference ΔR. Thereby, the required energy ΔE_M is measured. This energy is located in the field within the shell with center M, thickness ΔR and radius R, see Fig. (12). That shell has the volume

$$\Delta V = 4\pi R^2 \Delta R. \tag{112}$$

Consequently, the absolute value of the measured energy density is as follows:

$$|u_f| = \frac{\Delta E_M}{\Delta V} \tag{113}$$

The positive required energy compensates the energy of the field in the shell, as the field in the shell with volume ΔV is eliminated in the process of lifting the mass. Consequently, the sign of the field is negative:

$$u_f = -\frac{\Delta E_M}{\Delta V} \tag{114}$$

Alternatively, this measured energy can be calculated:

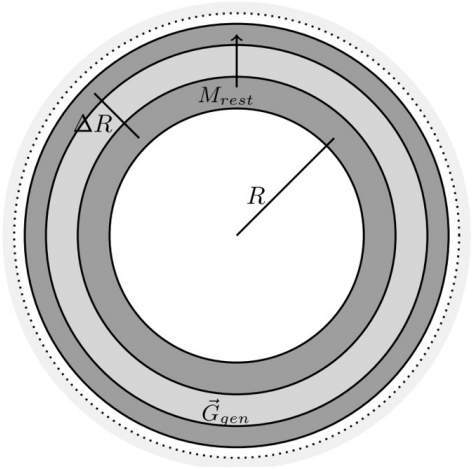

Figure 12: A mass M (dark gray) in a shell at a radius R is lifted to a radius $R+\Delta R$ as follows: Differential parts dM are lifted, while the rest M_{rest} is still at R. Thereby the field $\vec{G}_{gen} = \vec{G}^*$ (medium gray) in the shell with radius R and thickness ΔR becomes zero, when the whole mass is at $R + \Delta R$.

Derivation of the field's energy density: The required energy ΔE_M can be calculated, see Carmesin (2024a):

$$\Delta E_M = \frac{G \cdot M^2 \Delta R}{2R^2}. \tag{115}$$

The measured energy density in Eq. (114) can be calculated by inserting Eqs. (115 and 112) into Eq. (114):

$$u_f = -\frac{G \cdot M^2}{8\pi R^4} = -\frac{(\vec{G}^*)^2}{8\pi G} \tag{116}$$

For comparison, Peters (1981) derived the same formula for the energy density

$$u_f = -\frac{(\vec{G}^*)^2}{8\pi G}. \tag{117}$$

Peters (1981) derived this result in a Newtonian approximation.

In contrast, the exact energy density u_f is derived here. This is achieved with help of the exact field, since no approximation is used here. This exactness is achieved here with help of the distinction between the two distance measures: the gravitational parallax distance ΔR and the corresponding light travel distance ΔL.

Compensation of the negative field: The RGS in Eqs. (84 and 87) is divided by $8\pi G$, and $\vec{G}_{gen} = \vec{G}^*$ is used:

$$0 = \frac{\left(c \cdot \frac{\partial}{\partial \tau} \sum_{j \text{ in } \mathcal{S}} \varepsilon_{L,rr,j}\right)^2}{8\pi G} - \frac{(\vec{G}^*)^2}{8\pi G} \tag{118}$$

The sum in the above Eq. is identified with the summed relative additional volume of the indivisible VPs:

$$\varepsilon_{L,rr,indivisible\ VPs} := \sum_{j \text{ in } \mathcal{S}} \varepsilon_{L,rr,j} \tag{119}$$

With it, the RGS in Eq. (118) is as follows:

$$0 = \frac{c^2 \cdot \dot{\varepsilon}^2_{L,rr,indivisible\ VPs}}{8\pi G} + \frac{-(\vec{G}^*)^2}{8\pi G} \tag{120}$$

The second fraction in the above Eq. is identified with the energy density of the gravitational field u_f.

$$0 = \frac{c^2 \cdot \dot{\varepsilon}^2_{L,rr,indivisible\ VPs}}{8\pi G} + u_f \tag{121}$$

As a consequence, the fraction in the above Eq. is an energy density u. That fraction describes indivisible VPs δV_j that cause the field. Therefore, that fraction describes the energy density of the indivisible VPs δV_j:

$$u_{indivisible\ VPs} = \frac{c^2 \cdot \dot{\varepsilon}^2_{L,rr,indivisible\ VPs}}{8\pi G}. \tag{122}$$

Consequently, the sum of the two energy densities is zero:

$$u_{indivisible\ VPs} + u_f = 0. \tag{123}$$

The energy density of one indivisible VP is obtained by using $\vec{G}_{gen,j} = \vec{G}_j^*$ and by inserting the field in Eq. (83) into Eq. (117):

$$u_{f,j} = -\frac{(\vec{G}_j^*)^2}{8\pi G}. \tag{124}$$

Next, the rate gravity relation (see Eqs. 84 and 87) is generalized to one indivisible VP:

$$c^2 \dot{\varepsilon}^2_{L,rr,indivisible\ VP,j} = (\vec{G}_j^*)^2. \tag{125}$$

Similarly, Eq. (123) is generalized to one indivisible VP:

$$u_{indivisible\ VP,j} + u_{f,j} = 0. \tag{126}$$

With these generalizations, the energy density in Eq. (124) implies the energy density $u_{indivisible\ VP,j}$ of one indivisible VP δV_j as follows:

$$u_{indivisible\ VP,j} = -u_{f,j} = \frac{c^2 \cdot \dot{\varepsilon}^2_{L,rr,indivisible\ VP,j}}{8\pi G}. \tag{127}$$

These relations are results of the VD.

For comparison, expectation values of the field have been derived from the VD as follows: Firstly, a quantum field theory has been derived from the VD. Secondly, the expectation value of a field has been derived from the quantum field theory, see Carmesin (2024a, 2025e).

Each indivisible VP has the energy density $u_{indivisible\ VP,j}$ based on its rate. Moreover, each indivisible VP causes the energy density $u_{f,j}$ based on its gravity. Furthermore, each indivisible VP propagates at the speed c. Accordingly, such an indivisible VP can be called *rate gravity wave, RGW*.

8 Emergent quantum postulates

The VD, the dynamics of the indivisible VPs, implies the SEQ, the fundamental deterministic dynamics of quantum physics. Accordingly, the following question arises: Does the VD imply the stochastic dynamics of quantum systems and the complete system of quantum postulates?

In order to answer this question, the deterministic time evolution is summarized in a postulate, and mathematical consequences are derived first.

Then the stochastic dynamics and the complete system of the quantum postulates are derived.

Additional rules about mixed states and about entanglement in (Ballentine, 1998, p. 46) have been derived from the VD in Carmesin (2024a).

8.1 Deduction of the postulates

Postulate about the deterministic time evolution: The VD implies the postulate about the deterministic time evolution of quanta, see (Kumar, 2018, p. 170):

Postulate about the deterministic time evolution

'The time evolution of the state vector is governed by the time-dependent Schrödinger equation, SEQ, see (Schrödinger, 1926, Eq. (4")):

$$i\hbar\partial_t|\psi\rangle = \hat{H}|\psi\rangle, \tag{128}$$

where $\hat{H}$ is the Hamilton operator corresponding to the total energy of the system.' More generally, the VD implies the GSEQ.

On Hilbert space: In this section, the solution spaces of the SEQ and of the GSEQ are analyzed, in order to derive quantum postulates in later sections. In the corresponding paragraph, it is shown, that indivisible VPs can be described by the DEQ of VD, and that indivisible VPs as well as objects at the speed $v = c$ are described by the quantum physical GSEQ. In particular, objects with relatively small momentum, $\frac{p^2}{m_0^2c^2} << 1$, in leading order in $\frac{p^2}{m_0^2c^2}$, are described by the SEQ.

In this section, it is shown that the solutions of the SEQ, of the GSEQ and of the DEQ of VD form Hilbert spaces:

As usual, the Dirac notation is used: A wave function Ψ is expressed by a so-called ket $|\Psi\rangle$.

Moreover, two wave functions, $\Psi_1(\tau, \vec{L})$ and $\Psi_2(\tau, \vec{L})$, form a scalar product as follows:

$$\langle\Psi_1|\Psi_2\rangle = \int d^3L \Psi_1^*(\tau, \vec{L}) \cdot \Psi_2(\tau, \vec{L}) \tag{129}$$

Hereby, the superscript $*$ marks the complex conjugate value, this notation is nowadays usual in quantum physics, see e. g. Griffiths (1994), Ballentine (1998), Scheck (2013), Kumar (2018).

Based on that scalar product, a state $|\Psi\rangle$ is multiplied by a normalization factor t_n so that the following scalar product is equal to one:

$$\langle\Psi \cdot t_n|\Psi \cdot t_n\rangle = \int d^3r \Psi^*(\tau, \vec{L}) \cdot \Psi(\tau, \vec{L}) \cdot |t_n|^2 = 1 \tag{130}$$

Next, it is shown that these states form a Hilbert space $\mathcal{H}$:

The states $\Psi(\tau, \vec{L})$ form a **complete vector space**, as they are solutions of the (linear DEQ) SEQ. As a consequence, they form a linear vector space, whereby

they include all linear combinations of states $\Psi(\tau, \vec{L})$, including Fourier integrals, for instance. These form a complete Hilbert space $\mathcal{H}$, see e. g. (Teschl, 2014, p. 47) or (Sakurai and Napolitano, 1994, p. 57).

Generalization: The above derivation holds as well for the GSEQ, including rates of change tensors $\dot{\varepsilon}_{L,p} \cdot t_n$. Consequently, such wave functions form a Hilbert space as well.

Altogether, the solutions of the DEQ of volume dynamics (VD) form a Hilbert space $\mathcal{H}$, the solutions of the GSEQ form a Hilbert space $\mathcal{H}$, and the solutions of the SEQ form a Hilbert space $\mathcal{H}$. These DEQs and their respective Hilbert spaces, can describe VPs, indivisible VPs, matter, and radiation (the case of radiation is analyzed in Carmesin (2024a)).

On measurements, operators, and possible outcomes: In this section, the modeling of measurements with help of the above Hilbert space of the solutions of the deterministic dynamics of the GSEQ or of the SEQ is elaborated. This will be used in later sections in order to derive quantum postulates.

Firstly, the possible outcomes of a single measurement process are derived.

Secondly, the necessity of an additional dynamics is identified.

(1) In physics, in general, a measurement is described as follows:

(1.1) A measurable physical quantity A of an object is a function f of the mathematical description of that object.

(1.2) Thereby, a change of the state should be as small as possible.

(1.3) In general, the function f can be described in linear order by an operator $\hat{A}$ in Hilbert space, and by a Taylor series thereof: $f = \sum_{k=0}^{\infty} c_k \hat{A}^k$. Thereby, the zeroth order is not essential in physics. Thus, $f = \sum_{k=1}^{\infty} c_k \hat{A}^k$.

Therefore, a measurable physical quantity A of an object is described by a linear operator $\hat{A}$ in the Hilbert space of the states of the object.

(1.4) In the present case, the mathematical description is a state $|\Psi\rangle$ in a Hilbert space.

(1.5) In linear order in $\hat{A}$, the function applied to the state can be expressed as follows:

$$f_{linear}(|\Psi\rangle) = \hat{A}|\Psi\rangle, \quad \text{in linear order.} \tag{131}$$

(1.6) In general, each state $|\Psi\rangle$ can be expressed as a linear combination of eigenvectors $|\Psi_{A,n}\rangle$ with eigenvalues a_n. Here, the case of discrete and different eigenvalues a_n, each with one eigenvector, is analyzed in detail, as other cases can be analyzed analogously:

$$f_{linear}(|\Psi\rangle) = \hat{A}|\sum_n \Psi_{A,n}\rangle = \sum_n a_n |\Psi_{A,n}\rangle \tag{132}$$

(1.7) In order to keep the state unchanged in a single measurement process, see part (1.2), that process must act upon an eigenvector:

$$f_{linear}(|\Psi_{A,n}\rangle) = \hat{A}|\Psi_{A,n}\rangle = a_n|\Psi_{A,n}\rangle, \quad \text{single measurement process.} \tag{133}$$

Therefore, the outcome of a single measurement process of a quantity A of an object is one of the eigenvalues of the operator $\hat{A}$ corresponding to A.

(2) In general, a state is a linear combination of eigenvectors. But a possible outcome of each single measurement process is one of the eigenvalues. As a consequence, there must be a second dynamics that provides the choice of the eigenvalue that occurs in the measurement.

(2.1) The second dynamics cannot be deterministic, as the deterministic dynamics has been derived from mathematics in a very general manner, hence the derived deterministic dynamics is already very general. Thus, the only possibility for a very general second dynamics is a stochastic dynamics.

(2.2) Therefore, a general second dynamics must be a stochastic dynamics.

This stochastic dynamics is derived next:

On the stochastic dynamics: In this section, the stochastic dynamics is derived from the properties of the indivisible VPs.

(1) For the case of a single indivisible VP δV_j, the probability to measure an indivisible VP at an event $(\tau, \vec{L})$ is proportional to the energy density $u_{indivisible\ VP,j}$ of the indivisible VP δV_j at that event $(\tau, \vec{L})$.

(2) The energy density $u_{indivisible\ VP,j}$ is related to the wave function as follows:

(2.1) For the case of a single indivisible VP δV_j, the wave function is the time derivative of its relative additional volume, multiplied by a normalization factor t_n:

$$|\Psi_{indivisible\ VP\ j}\rangle = t_n \cdot \dot{\varepsilon}_{indivisible\ VP\ j}. \tag{134}$$

(2.2) The absolute square is applied to the above equation:

$$|\Psi^2_{indivisible\ VP\ j}|$$

$$= \langle \Psi_{indivisible\ VP\ j} | \Psi_{indivisible\ VP\ j} \rangle$$
$$= t_n^2 \cdot \dot{\varepsilon}^2_{indivisible\ VP\ j}. \quad (135)$$

(2.3) The above equation is multiplied by $1 = \frac{8\pi G}{c^2} \cdot \frac{c^2}{8\pi G}$:

$$|\Psi^2_{indivisible\ VP\ j}| = \frac{8\pi G}{c^2} t_n^2 \cdot \frac{c^2 \dot{\varepsilon}^2_{indivisible\ VP\ j}}{8\pi G}. \quad (136)$$

(2.4) In the above equation, the second fraction is identified with the energy density of the indivisible VP δV_j:

$$|\Psi^2_{indivisible\ VP\ j}| = \frac{8\pi G}{c^2} t_n^2 \cdot u_{indivisible\ VP\ j}. \quad (137)$$

(3) As a consequence, the probability $P_{indivisible\ VP\ j}$ to measure an indivisible VP at an event $(\tau, \vec{L})$ is proportional to the absolute square of the wave function:

$$P_{indivisible\ VP\ j} \propto |\Psi^2_{indivisible\ VP\ j}|. \quad (138)$$

(4) For each measurable quantity A, and for the corresponding operator $\hat{A}$, the probability to measure an eigenvalue a_n of an eigenvector $|\Psi_{A,n}\rangle$ has been derived from the result in part (3) or in Eq. (138), see Carmesin (2024a).

Therefore, the result in part (3) or in Eq. (138) is the fundamental stochastic dynamics of quantum physics.

(5) As a consequence, the VD implies both, deterministic time evolution as well as the stochastic dynamics of quantum physics. Consequently, the VD implies the full dynamics of quantum physics[3].

Using the above mathematical results as well as the deterministic and stochastic dynamics, the postulates of quantum physics are derived next:

Derivation of the postulates: In this section, it is shown how the quantum postulates in Kumar (2018) are implied by the VD:

(1) The postulate about the **deterministic time evolution** has been derived.

(2) The postulate about **probabilistic outcomes of measurements** is as follows, see (Kumar, 2018, p. 169, 170):

[3]This includes quantum field theory and the Dirac theory, as both can be derived with help of the above deterministic and stochastic dynamics, see e. g. Sakurai and Napolitano (1994), Carmesin (2022b, 2023, 2024a, 2025e).

'If a measurement of an observable A is made in a state $|\Psi(t)\rangle$ of the quantum mechanical system, then the following holds:

[1] The probability of obtaining one of the non-degenerate discrete eigenvalues a_j of the corresponding operator $\hat{A}$ is given by

$$P(a_j) = \frac{|\langle \phi_j | \Psi \rangle|^2}{\langle \Psi | \Psi \rangle}, \quad (139)$$

where $|\phi_j\rangle$ is the eigenfunction of $\hat{A}$ with the eigenvalue a_j. If the state vector is normalized to unity, $P(a_j) = |\langle \phi_j | \Psi \rangle|^2$.

[2] If the eigenvalue a_j is m_j-fold degenerate, this probability is given by

$$P(a_j) = \frac{\Sigma_{i=1}^{m_j} |\langle \phi_{j,i} | \Psi \rangle|^2}{\langle \Psi | \Psi \rangle}, \quad (140)$$

[3] If the operator $\hat{A}$ possesses a continuous spectrum $\{a\}$, the probability that the result of a measurement will yield a value between a and $a + da$ is given by

$$P(a) = \frac{|\langle \phi(a) | \Psi \rangle|^2}{\langle \Psi | \Psi \rangle} \cdot da$$
$$= \frac{|\langle \phi(a) | \Psi \rangle|^2}{\int_{-\infty}^{\infty} |\Psi(a')|^2 da'} \cdot da \quad (141)$$

This postulate can be derived from the stochastic dynamics. The derivation is presented in Carmesin (2022b,a, 2024a).

(3) The postulate about **Hilbert space** is as follows, see (Kumar, 2018, p. 168):

'The state of a quantum mechanical system, at a given instant of time, is described by a vector $|\Psi(t)\rangle$, in the abstract Hilbert space $\mathcal{H}$ of the system.'

For each given state of a quantum mechanical system, the full dynamics should be determined. It is the deterministic and stochastic dynamics in the above postulates (1) and (2). It has been shown here, that the states of the respective Hilbert space provide the full information to derive the deterministic time evolution (with the SEQ or with the GSEQ, more generally), and to derive the correct probabilities for the probabilistic outcomes. Therefore, 'the state of a quantum mechanical system, at a given instant of time, is described by a vector $|\Psi(t)\rangle$, in the abstract Hilbert space $\mathcal{H}$ of the system'.

Moreover, it is insightful to realize that the correct probabilistic outcomes are a consequence of the gravitational properties of the VD. Therefore, it is enlightening to understand that the basis of the quantum postulates is a quantum gravitational foundation.

As a consequence, **a deep and fundamental understanding of quantum physics without understanding gravity and quantum gravity is hardly possible**.

(4) The postulate about the **relation between observables and operators** is as follows, see (Kumar, 2018, p. 169):

'A measurable physical quantity A (called an observable or dynamic physical quantity), is represented by a linear and hermitian operator $\hat{A}$ acting in the Hilbert space of state vectors.'

This postulate is founded by the VD.

(5) The postulate about the relation between the possible **outcomes of a measurement and the eigenvalues** is as follows, see (Kumar, 2018, p. 169):

'The measurement of an observable A in a given state may be represented formally by the action of an operator $\hat{A}$ on the state vector $|\Psi(t)\rangle$. The only possible outcome of such a measurement is one of the eigenvalues, $\{a_j\}, j = 1, 2, 3, \ldots,$ of $\hat{A}$.'

This postulate is founded by the VD.

8.2 Analysis of the formal derivation of the Schrödinger equation and quantum postulates

In this section, the above formal derivation of the Schrödinger equation and quantum postulates is analyzed. Thereby, the properties of the volume portions are worked out, that imply quantum physics, gravity and relativity in a unifying manner, see also Fig. (20).

(1) The **Space Paradox** is derived from founded experimental results.

(2) The Space Paradox implies, that **indivisible volume portions** form space as a stochastic average. In order to solve the Space Paradox, the dynamics of the indivisible volume portions is analyzed as follows:

(3) The **differential Eq. (DEQ) of the propagation** of the relative additional volume ε_L of indivisible volume portions is derived from the total derivative. As the total derivative is a very reliable mathematical fact, the resulting DEQ of the propagation is very founded.

(4) A **dynamics underlying the relative additional volume** ε_L of indivisible is derived. For it, the time derivative is applied to the DEQ of the propagation. As a consequence, the dynamics of the time derivative $\dot{\varepsilon}_L$ of the relative additional volume is derived. The square of $\dot{\varepsilon}_L$, multiplied by $\frac{c^2}{8\pi G}$ is identified with the energy density $u_{indivisible\,VP} = \frac{c^2 \dot{\varepsilon}_L^2}{8\pi G}$ of the gravitational field that is inherent to ε_L. Consequently, $\dot{\varepsilon}_L$ is proportional to the square root of the energy density of the relative additional volume ε_L. Therefore, the dynamics of $\dot{\varepsilon}_L$ is essentially underlying the physics of the indivisible VP: $\dot{\varepsilon}_L$ represents a derivative and a root (multiplied by a constant) of the energy density of ε_L.

(5) Essential properties of the underlying dynamics in item (4) are derived: The DEQ of that dynamics is a generalized **Schrödinger Eq.**, which implies the usual Schrödinger (1926) equation. Moreover, the wave function in the Schrödinger Eq. (SEQ) is identified with the normalized version $t_n \cdot \dot{\varepsilon}_L$ of $\dot{\varepsilon}_L$. Therefore, the **wave function is explained and derived**, this result is not provided by present - day quantum physics, see Scheck (2013).

(6) As the derived SEQ is a linear DEQ, its solutions form a linear vector space. That vector space is identified with the **Hilbert space** in quantum physics.

(7) The energy density $u_{indivisible\,VP} = \frac{c^2 \dot{\varepsilon}_L^2}{8\pi G}$ implies the **probabilistic dynamics of quanta**, that has already been observed in many experiments, and that is summarized in the respective **quantum postulate about the probabilistic dynamics**.

(8) As the derived wave functions $\Psi = t_n \cdot \dot{\varepsilon}_L$ fulfill the correct deterministic dynamics, the SEQ, and as Ψ fulfills the correct probabilistic dynamics of quanta, these wave functions Ψ represent the **quantum states**.

(9) The items (4-8) imply the **quantum postulates**.

(10) Furthermore, the Schwarzschild metric is derived from the dynamics of the volume portions.

(11) Moreover, from these postulates, the quantum physics of mixed state, the Dirac equqtion, and the quantum field theory can be developed, see Sakurai and Napolitano (1994), Ballentine (1998).

Altogether, results (1-10) are derived here in a formal and straight manner. Thereby, the five important properties of volume portions are derived and they are essential:

an indivisible volume portion is not the sum of parts,

the DEQ of volume dynamics describes indivisible volume portions,

indivisible volume portions have the gravitational property,

indivisible volume portions can curve space and time,

indivisible volume portions fulfill the quantum postulates.

Therefore these five properties form an impartible characterization of cosmological space, and of

the indivisible volume portions that form cosmological space as a stochastic average, and that imply the quantum properties.

9 Prediction of the ACS and of time

In this section, the solution of the problem of finding an ACS is completed by predicting the velocity of the ACS at each point in the universe. Moreover, that velocity of the ACS of space and time provides the kinematic time difference as well as its fluctuation and its time evolution.

9.1 Expectation values

In this section, we generalize the concept of adequate frames with help of the wave function ψ.

Wave function near celestial bodies: For each celestial body C_i, the wave function ψ_i is derived. For it, the field $\vec{G}^*_{exact,i}$ caused by C_i at an event $(\tau, \vec{L})$ is expressed in terms of its indivisible field parts, see Eq. (80):

$$\vec{G}^*_{exact,i}(\tau,\vec{L}) = \sum_{j\ in\ \mathcal{S}} \vec{G}_{i,j}(\tau,\vec{L})$$
$$\text{with}\quad \vec{G}_{i,j}(\tau,\vec{L}) := c^2 \frac{\partial}{\partial \vec{L}} \varepsilon_{L,rr,i,j} \tag{142}$$

For instance, an event $(\tau, \vec{L})$ can be marked by a clock C measuring its own time and position. Next, the direction vector $\vec{e}_{r_{i,j}}$ is applied, and the event $(\tau, \vec{L})$ is not explicated, for short:

$$\vec{G}_{i,j} = -c^2 \frac{\partial}{\partial L} \varepsilon_{L,rr,i,j} \cdot \vec{e}_{r_{i,j}} \tag{143}$$

Hereby, $\vec{e}_{r_{i,j}}$ is the radial unit vector, and we used the fact that $\varepsilon_{L,rr,i,j}$ decreases as a function of $L = |\vec{L}|$. We substitute $\frac{\partial}{\partial L} = \frac{\partial \tau}{\partial L}\frac{\partial}{\partial \tau}$:

$$\vec{G}_{i,j} = -c^2 \frac{\partial \tau}{\partial L}\frac{\partial}{\partial \tau} \varepsilon_{L,rr,i,j} \cdot \vec{e}_{r_{i,j}} \tag{144}$$

We use $\frac{\partial \tau}{\partial L} = \frac{1}{\frac{\partial L}{\partial \tau}} = \frac{1}{c}$ and $\frac{\partial \varepsilon_{L,rr,i,j}}{\partial \tau} = \dot{\varepsilon}_{L,rr,i,j}$:

$$\vec{G}_{i,j} = -c \dot{\varepsilon}_{L,rr,i,j} \cdot \vec{e}_{r_{i,j}} \tag{145}$$

We identify the normalized wave function of $\Psi_{i,j} := t_n \cdot \dot{\varepsilon}_{L,rr,i,j}$ of the field $\vec{G}_{i,j}$, see Eq. (64), as well as the non - normalized wave function $\psi_{i,j} := \dot{\varepsilon}_{L,rr,i,j}$:

$$\vec{G}_{i,j} = -c \psi_{i,j} \vec{e}_{r_{i,j}} \tag{146}$$

These indivisible field parts are inserted in Eq. (142):

$$\vec{G}^*_{exact,i}(\tau,\vec{L}) = -c \sum_{j\ in\ \mathcal{S}} \psi_{i,j} \vec{e}_{r_{i,j}}(\tau,\vec{L}) \tag{147}$$

In the following, $\vec{G}^*_{exact,i}$ is sometimes denoted by $\vec{G}^*_i$, for short. The sum in the above Eq. is identified with a corresponding product of a wave function ψ_i and a direction vector $\vec{e}_{r_i}$:

$$\vec{G}^*_{exact,i}(\tau,\vec{L}) = -c\psi_i \vec{e}_{r_i}(\tau,\vec{L})$$
$$\text{with}\quad \psi_i \vec{e}_{r_i} := \sum_{j\ in\ \mathcal{S}} \psi_{i,j} \vec{e}_{r_{i,j}} \tag{148}$$

Expectation value of the velocity: Next, the expectation value $\langle \vec{v}_C \rangle$ of the velocity $\vec{v}_C$ of a clock C at an event $(\tau, \vec{L})$ in the vicinity of N celestial bodies C_i is derived.

As a consequence of Eq. (148), the field of the celestial bodies represents their wave function as follows:

$$\vec{G}^* = \sum_{i=1}^{i=N} \vec{G}^*_{exact,i} = -c \sum_{i=1}^{i=N} \psi_i \vec{e}_{r_i} \tag{149}$$

Consequently, the expectation value of the velocity is as follows:

$$\langle \vec{v}_C \rangle = \frac{\langle \sum_{k=1}^{k=N} \psi_k \vec{e}_{r_k} \hat{\vec{v}}_C \sum_{i=1}^{i=N} \psi_i \vec{e}_{r_i} \rangle}{\langle \sum_{k=1}^{k=N} \psi_k \vec{e}_{r_k} | \sum_{i=1}^{i=N} \psi_i \vec{e}_{r_i} \rangle} \tag{150}$$

The above products of sums are evaluated:

$$\langle \vec{v}_C \rangle = \frac{\sum_{k=1}^{k=N} \sum_{i=1}^{i=N} \langle \psi_k \vec{e}_{r_k} \hat{\vec{v}}_C \psi_i \vec{e}_{r_i} \rangle}{\sum_{k=1}^{k=N} \sum_{i=1}^{i=N} \langle \psi_k \vec{e}_{r_k} | \psi_i \vec{e}_{r_i} \rangle} \tag{151}$$

The above velocity $\vec{v}_C$ can be measured, as shown above. As a consequence, the velocity has been expressed by an eigenvalue generating operator $\hat{\vec{v}}_C$, see e. g. Kumar (2018), Carmesin (2024a). Thereby, the eigenvalue is the velocity $\vec{v}_{C\ relative\ to\ \vec{G}^*_i}$, shortly $\vec{v}_{C,\ \underline{\vec{G}^*_i}}$ of the clock C relative to the field of the wave function:

$$\hat{\vec{v}}_C |\psi_i \vec{e}_{r_i}\rangle = \vec{v}_{C,\ \underline{\vec{G}^*_i}} |\psi_i \vec{e}_{r_i}\rangle \tag{152}$$

Therefore, the expectation value in Eq. (151) is as follows:

$$\boxed{\langle \vec{v}_C \rangle = \frac{\sum_{k=1}^{k=N} \sum_{i=1}^{i=N} \langle \psi_k \vec{e}_{r_k} | \vec{v}_{C,\ \underline{\vec{G}^*_i}} | \psi_i \vec{e}_{r_i} \rangle}{\sum_{k=1}^{k=N} \sum_{i=1}^{i=N} \langle \psi_k \vec{e}_{r_k} | \psi_i \vec{e}_{r_i} \rangle}} \tag{153}$$

In many cases, the field can be measured or derived. Correspondingly, the product $\psi_k \vec{e}_{r_k}$ in the Hilbert space vector $\langle \psi_k \vec{e}_{r_k}|$ can be substituted by the field according to Eq. (148). Thereby, the factor $-c$ cancels out. Therefore, the expectation value is as follows:

$$\boxed{\langle \vec{v}_C \rangle = \frac{\sum_{k=1}^{k=N} \sum_{i=1}^{i=N} \vec{G}_k^* \cdot \vec{G}_i^* \cdot \vec{v}_{C,\, \underline{\vec{G}_i^*}}}{\sum_{k=1}^{k=N} \sum_{i=1}^{i=N} \vec{G}_k^* \cdot \vec{G}_i^*}} \qquad (154)$$

A possible approximation: If the fields $\vec{G}^*_{exact,i}$ and $\vec{G}^*_{exact,k}$ of the two celestial bodies are very small, then the wave functions ψ_i and ψ_k of two different celestial bodies C_i and C_k are approximately (stochastically) independent of each other, and they do hardly interact with each other. This approximation might be adequate for the case of very distant celestial bodies, or for the case of planetesimals, see Karttunen et al. (2007), or for the case of particles of dust or molecules or atoms, for instance.

In that approximation, these wave functions are orthogonal to each other in Hilbert space $\mathcal{H}$. Consequently, the expectation value in Eq. (153) is as follows:

$$\langle \vec{v}_C \rangle = \frac{\sum_{k=1}^{k=N} \vec{v}_{C,\, \underline{\vec{G}_k^*}} \langle \psi_k \vec{e}_{r_k} | \psi_k \vec{e}_{r_k} \rangle}{\sum_{k=1}^{k=N} \langle \psi_k \vec{e}_{r_k} | \psi_k \vec{e}_{r_k} \rangle} \qquad (155)$$

Each of the above brackets is equal to the square of the corresponding field divided by c^2, see Eq. (146). As a consequence, the expectation value in Eq. (155) is as follows:

$$\boxed{\langle \vec{v}_C \rangle = \frac{\sum_{k=1}^{k=N} \vec{v}_{C,\, \underline{\vec{G}_k^*}} \cdot (\vec{G}_k^*)^2}{\sum_{k=1}^{k=N} (\vec{G}_k^*)^2}} \qquad (156)$$

9.2 Fluctuations of time

In this section, the expectation value of the fluctuation of time is analyzed and calculated.

Calculation of the velocity relative to the ACS: At each point P, there are fields $\vec{G}_k^*$ of the objects C_k that dominate gravity at P. As a consequence, a clock C near P has the expectation value $\langle \vec{v}_C \rangle$ of its velocity in Eq. (154). That Eq. (154) represents the expectation value of the eigenvalues of the velocity relative to the dominating fields $\vec{G}_k^*$. As the velocity relative to the field is the same as the velocity relative to the ACS, the expectation value in Eq. (154) is the expectation value of the velocity of the clock relative to the local ACS:

$$\langle \vec{v}_C \rangle = \langle \vec{v}_{C,\underline{ACS}} \rangle \qquad (157)$$

Therefore, for each point P and each clock C near P, the expectation value in Eq. (154) is the quantum physical best determination of the velocity of the clock relative to the ACS:

$$\langle \vec{v}_C \rangle = \text{best determination of } \vec{v}_{C,\underline{ACS}} \qquad (158)$$

Kinematic time difference as a function of speed: For each point P and each clock C near P, the expectation value of its velocity $\vec{v}_{C,\underline{ACS}}$ relative to the ACS at P is the expectation value in Eq. (154). As a consequence of the definition of the ACS, the velocity $\vec{v}_{C,\underline{ACS}}$ relative to the ACS provides the kinematic fractional time difference $\delta t_{kin,frac}$ according to the relativity formula as a function of $\vec{v}_{C,\underline{ACS}}$:

$$\delta t_{kin,frac}(v_{C,\underline{ACS}}) = -\frac{\langle \vec{v}_{C,\underline{ACS}} \rangle^2}{2c^2} \qquad (159)$$

As the velocity is squared, $\delta t_{kin,frac}$ is a function of the speed $|\vec{v}_{C,\underline{ACS}}| =: v_{C,\underline{ACS}}$.

Clock with minimal speed in the ACS: For each point P and each clock C near P, the expectation value of its velocity $\vec{v}_{C,\underline{ACS}}$ relative to the ACS at P is the expectation value $\langle \vec{v}_C \rangle$ in Eq. (154).

Therefore, the best calculable and applicable value for $\vec{v}_{C,\underline{ACS}}$ is $\langle \vec{v}_C \rangle$.

Consequently, the best calculable minimal speed of the clock is the difference of the velocity $\vec{v}_{C,\underline{ACS}}$ and the best calculable value $\langle \vec{v}_C \rangle$:

$$|\vec{v}_{C,min}| = |\vec{v}_{C,\underline{ACS}} - \langle \vec{v}_C \rangle| \qquad (160)$$

Clock with maximal kinematic time difference: As shown above, for each point P, and for each clock C near P, the clock's minimal speed in the ACS is given in Eq. (160). As a consequence of the definition of the ACS, that minimal speed provides the maximal kinematic time difference as follows:

$$\delta t_{kin,frac,max} = -\frac{\vec{v}^2_{C,min}}{2c^2} \qquad (161)$$

The maximal mathematically possible kinematic time difference is zero, as the above Eq. represents a parabola with its maximum at the origin. Insertion of the minimal velocity in Eq. (160) yields the maximal kinematic time difference as follows:

$$\delta t_{kin,frac,max} = -\frac{(\vec{v}_C - \langle \vec{v}_C \rangle)^2}{2c^2} \qquad (162)$$

Consequently, the expectation value of the maximal kinematic time difference as follows:

$$\langle \delta t_{kin,frac,max} \rangle = -\frac{\langle (\vec{v}_C - \langle \vec{v}_C \rangle)^2 \rangle}{2c^2} \text{ or}$$

$$\langle \delta t_{kin,frac,max} \rangle = -\frac{\langle \vec{v}_C^2 \rangle - \langle \vec{v}_C \rangle^2}{2c^2} \quad (163)$$

It is the squared standard deviation $\sigma_{v_c}^2$ of v_C divided by $-2c^2$:

$$\langle \delta t_{kin,frac,max} \rangle = -\frac{\sigma_{v_c}^2}{2c^2}$$
$$\text{with} \quad \sigma_{v_c}^2 := \langle \vec{v}_C^2 \rangle - \langle \vec{v}_C \rangle^2 \quad (164)$$

Interpretation: This expectation value of the kinematic fractional time difference $\langle \delta t_{kin,frac,max} \rangle$ is caused by the superposition of different gravitational fields or field parts, caused by masses or dynamic masses moving at different velocities. Accordingly, this kinematic time difference is caused by such fluctuations of the gravitational field at the considered point P. As each gravitational field part is proportional to a respective wave function, this expectation value of the kinematic fractional time difference $\langle \delta t_{kin,frac,max} \rangle$ is caused by such quantum fluctuations.

It is emphasized that $\langle \delta t_{kin,frac,max} \rangle$ is a special type of time fluctuations. It is not excluded that there might occur other time fluctuations additionally.

9.3 Increasing precision of time

In this section, it is shown that the expectation value of the kinematic fractional time difference $\langle \delta t_{kin,frac,max} \rangle$ was very large in the early universe, whereas it is very small in the present - day universe. Therefore, it is shown that the precision of time increases during the time evolution of the universe, and correspondingly, these quantum fluctuations decrease during the time evolution of the universe.

In the early universe, after the emission of the CMB, the universe was filled with a gas of hydrogen atoms at a temperature of ca. $T = 3000\,\mathrm{K}$, Unsöld and Baschek (1999). As a consequence of the Maxwell distribution in a gas, see Landau and Lifschitz (1980) §29, a gas with a temperature T and consisting of particles, each with a mass $m_H = 1.6738 \cdot 10^{-27}\,\mathrm{kg}$, has the following expectation value of the squared velocity:

$$\langle v^2 \rangle = \frac{k_B \cdot T}{m} = 2.47 \cdot 10^7 \,\frac{\mathrm{m}}{\mathrm{s}} = \sigma_v^2 \quad (165)$$

Hereby, as the expectation value of the velocity of the gas is zero, this value is also the squared standard deviation σ_v^2 of the velocity. As there is no huge dominating mass in this gas in the early universe, this squared standard deviation σ_v^2 additionally represents the squared speed relative to the ACS. As a consequence, the expectation value of the kinematic fractional time difference $\langle \delta t_{kin,frac,max} \rangle$ caused by these quantum fluctuations (see Eq. 164) is as follows:

$$\langle \delta t_{kin,frac,max} \rangle = -\frac{\sigma_v^2}{2c^2} = -1.37 \cdot 10^{-10} \quad (166)$$

In contrast, in the vicinity of celestial bodies, the expectation value of the maximal kinematic fractional time difference in Eq. (164) has typical absolute values in the range 10^{-14} to 10^{-17}, see Fig. (13).

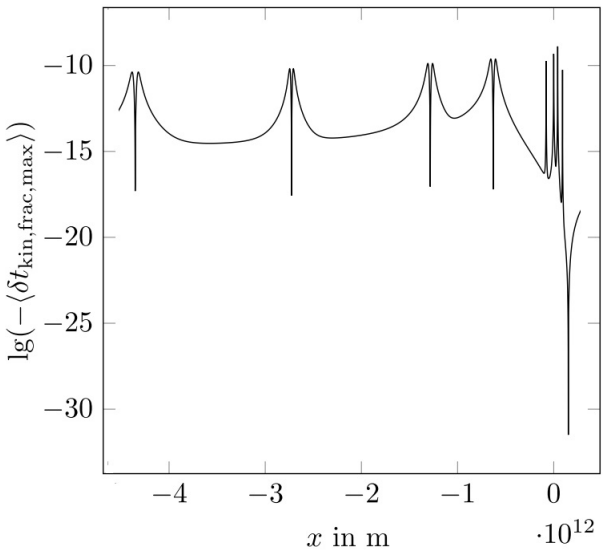

Figure 13: Fluctuations at the planets: logarithm with basis 10 of the negative expectation value of the kinematic fractional time difference $\langle \delta t_{kin,frac,max} \rangle$ as a function of the location x with $x = 0$ at Earth. At each planet, there is a local minimum surrounded by a region of relatively large values of that logarithm. In this constellation, the planets and Sun are in a linear row, from left to right: Neptune, Uranus, Saturn, Jupiter, Mars, Earth, Venus, Mercury and Sun with a deep minimum. At this scale, the minima are not visible for the planets Mars, Earth, Venus, Mercury.

These two examples show the following:

During the time from the emission of the CMB until today, the expectation value of the kinematic fractional time difference $\langle \delta t_{kin,frac,max} \rangle$ decreased by a factor 10^4 or more. Correspondingly, these quantum fluctuations of the time decreased by that factor. Consequently, the time started with relatively large fluctuations that decreased during the time evolution of the universe. This is caused by the increase of heterogeneity during the time evolution of the universe.

9.4 Interpretation of the constellation of planets

The constellation of the planets in one line in Fig. (13) is artificial. It has been chosen, in order to present the planets, their surroundings, and the respective time fluctuations as a function of the distance to Earth in a two-dimensional graph.

In this graph, the absolute expectation value of the kinematic fractional time difference $|\langle \delta t_{kin,frac,max} \rangle|$ = $|-\frac{\langle v^2 \rangle - \langle v \rangle^2}{2c^2}|$ is shown at a logarithmic scale. In the vicinity of a single or very dominant celestial body, this $|\langle \delta t_{kin,frac,max} \rangle|$ is almost zero, this is the case in the vicinity of Sun, see Fig. (13).

At other places in our planetary system, the superposition of gravitational fields of different celestial bodies is essential. This causes an increase of $|\langle \delta t_{kin,frac,max} \rangle|$, as the fluctuations $|-\frac{\langle v^2 \rangle - \langle v \rangle^2}{2c^2}|$ do increasingly deviate from zero, see Fig. (13).

Thereby, in the vicinity of a planet, there occur two effects: In the very near vicinity of a planet, the gravitational field of that planet becomes very dominant, and this causes a decrease of absolute fluctuations $|\langle \delta t_{\mathrm{kin,frac,max}}|$, see Fig. (13). In the farther vicinity of a planet, the gravitational field of the planet and of Sun superimpose significantly. This causes relatively large absolute fluctuations $|\langle \delta t_{\mathrm{kin,frac,max}}|$, see Fig. (13). For the case of the outer planets, the region of such fluctuations is relatively large, whereas in the case of the inner planets, the range of these effects is relatively small, as the gravitational field of Sun is very large and tends to dominate.

Altogether, in Fig. (13), these effects can be compared for all planets in one graph.

10 Comparison with post-Newtonian parameters

Phenomena of gravity and relativity have been modeled with help of parameters in so-called post-Newtonian parameter (PPN) descriptions, see e. g. Chandrasekhar (1965), Will (2014), Liu and Liao (2024), Losada et al. (2025). Such parameters can be fitted experimentally. In the present theory, the fundamental physical constants G, c and $\hbar$ are used. With it, the theory of gravity is derived without any approximation and without any execution of a parameter fit. Therefore, it is interesting to compare a PPN description with the present theory. This will be done for few examples. The comparison of further examples is planned in a future paper.

(1) For instance, the squared line element ds^2 in Eq. (2) has been investigated with help of PPN parameters as follows, see Losada et al. (2025), Eq. (1):

$$ds^2 = g_{tt}c^2dt^2 + g_{rr}dr^2 + r^2 d\Omega \tag{167}$$

Thereby, spherical polar coordinates are used, and $r^2 d\Omega$ represents the differential of the two-dimensional subspace orthogonal to dr. In the PPN formalism, the tensor elements are as follows:

$$g_{tt} = 1 - \frac{2GM}{c^2 r} + \frac{2G^2M^2(\beta_{PPN} - \gamma_{PPN})}{c^4 r^2}$$
$$-g_{rr} = \frac{1}{1 - \frac{2GM}{c^2 r}} \doteq 1 + \frac{2GM}{c^2 r} \tag{168}$$

Hereby, β_{PPN} and γ_{PPN} are parameters that have to be investigated. An observation of the orbits of the stars S2 and S62 near the galactic center provides the parameter estimation or parameter fit, see Losada et al. (2025)

$$\gamma_{PPN} = 1 \pm 0.012 \text{ and } \beta_{PPN} = 1 \pm 0.02. \tag{169}$$

With $\gamma_{PPN} = 1 = \beta_{PPN}$, Eq (168) is as follows:

$$g_{tt} = \left(1 - \frac{2GM}{c^2 r}\right)$$
$$-g_{rr} \doteq 1 + \frac{2GM}{c^2 r} \tag{170}$$

This are the respective tensor elements of the present theory. Consequqntly, the present theory is in accordance with the result of Losada et al. (2025).

(2) From the squared line element in (1), the time dilation can be derived, and this can be interpreted with help of the ACS of the present theory. For it, Eqs. (10, 11, 12) of the present theory are used:

$$\Phi(r) = -\frac{GM}{r}. \tag{171}$$

This term represents a Newtonian potential. Additionally this term represents exact gravity in the framework of the derived theory of emergent gravity (thereby, lengths of curved space are used for light travel distances).

$$g_{tt} = g_{00} = 1 - \frac{2|\Phi|}{c^2}. \tag{172}$$

$$d\tau = dt \cdot \sqrt{1 - \frac{2|\Phi|}{c^2} - \frac{v^2}{c^2}}, \quad \text{near a mass.} \tag{173}$$

The present theory clarifies the meaning of the velocity v in the above equation: It is the velocity relative to the ACS. This is an additional advantage of the present theory. For comparison, usually, the purpose of the PPN description is to study the effect of parameters upon observable quantities.

(3) As another example, the Hubble tension is analyzed, see Riess (2022), Liu and Liao (2024). The basic model of cosmolgy is the ΛCDM - model, see e. g. Planck-Collaboration (2020). In that model, the Hubble constant H_0 of the universe should have a constant value. However, observation shows that the value in the early universe, obtained by the cosmic microwave background (CMB), see Planck-Collaboration (2020), differs significantly from the value in the late universe at the five σ confidence level, see Riess (2022), Galbany (2023).

In the PPN framework, the above Eq. (168) is approximated at linear order for $\frac{2|\Phi|}{c^2} \ll 1$:

$$g_{tt} = 1 - 2\underbrace{\frac{GM}{c^2 r}}_{\Psi_{PPN}} \quad \text{and} \quad -g_{rr} \doteq 1 + 2\underbrace{\frac{GM}{c^2 r}}_{\Phi_{PPN}} \tag{174}$$

Thereby, in the PPN description, the two parameters Ψ_{PPN} and Φ_{PPN} are introduced as values for the above indicated terms. In the PPN framework, the ratio of these parameters is an additional parameter

$$\gamma_{PPN} = \frac{\Phi_{PPN}}{\Psi_{PPN}}. \tag{175}$$

Gravitational lenses can simultaneously constrain this parameter γ_{PPN} and the values of H_0, see Losada et al. (2025). This does not yet explain the Hubble tension.

For comparison, an advantage of the present theory and of the exact gravitational potential of emergent gravity used in that theory is as follows: That theory explains and derives the Hubble tension in precise accordance with observation within the errors of measurement. Thereby, no fit is executed, and no unfounded hypothesis is used or proposed, see the path of derivation in Fig. (20) and e. g. Carmesin (2025e).

Altogether, the present theory uses emergent gravity with an exact potential, and relativity with a derived ACS. On that basis, several results have been achieved, and this substantiates the effectiveness of the exact potential:

(1) An explanation and derivation of the PPN parameters $\gamma_{PPN} = 1$ and $\beta_{PPN} = 1$ is provided, and it is in accordance with the observation by Losada et al. (2025).

(2) The PPN parameters $\gamma_{PPN} = 1$ and $\beta_{PPN} = 1$ are inherent to the Eq. of time dilation (Eq. 173), and the meaning of the velocity in that Eq. is explained and derived here: v is the velocity relative to the ACS.

(3) An explanation and derivation of the Hubble tension is provided, see e. g. Carmesin (2025e).

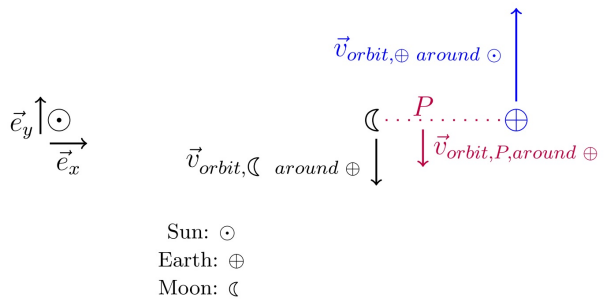

Figure 14: A possible journey from Earth to the Moon is sketched. Thereby, a constellation with Sun, Moon and Earth in a straight line is investigated. Hereby, a Sun Centered Inertial (SCI) coordinate system is used.
In this journey, the spacecraft moves at the straight line from Earth to Moon. Each point P on that straight line moves.
The SCI system is marked by two direction vectors $\vec{e}_x$ and $\vec{e}_y$. The velocities of Earth $\vec{v}_{orbit,\oplus\ around\ \odot}$, of the Moon $\vec{v}_{orbit,\leftmoon\ around\ \oplus}$ and of P, $\vec{v}_{orbit,P\ around\ \oplus}$, are marked by vectors. The velocity of the ACS, $\vec{v}_{ACS,\underline{SCI}}$, is a linear combination of $\vec{v}_{orbit,\oplus\ around\ \odot}$ and $\vec{v}_{orbit,\leftmoon\ around\ \oplus}$. Consequently, $\vec{v}_{ACS,\underline{SCI}}$ is parallel to $\vec{e}_y$, and the corresponding speed $|v_{ACS,\underline{SCI}}|$ is shown in Fig. (16).

11 An Artemis Moon mission prediction

The NASA plans to build a sustained station on the Moon in the so-called Artemis Moon mission NASA (2022), taking place from 2022 to 2030 and beyond.

In that mission, the kinematic time difference in the space between Earth and Moon can be investigated. With it, the present theory can be tested. As the precise routes and times of the spaceflights of the Artemis mission are not known in advance, a possible journey from Earth to the Moon is investigated here as an example:

11.1 Trajectory models

Two trajectory models are investigated here:

(1) $\odot$-$\leftmoon$ -$\oplus$-line:

In this trajectory model, Sun, Moon and Earth are at a straight line, see Fig. (14).

The journey takes place at the straight line from Earth to the Moon. For each point P of that straight line, the velocity of the ACS, $\vec{v}_{ACS,\underline{SCI}}$ is derived. Hereby

and in this section, the approximation in Eq. (156) has been used:

(1.1) The velocity of the ACS, $\vec{v}_{ACS,\underline{SCI}}$, relative to the SCI is equal to the expectation value $\langle \vec{v}_C \rangle$ of a clock in Eq. (156). In this expectation value $\langle \vec{v}_C \rangle$, for each celestial body k, the velocity $\vec{v}_{C,\,\vec{G}_k^*}$ (which describes the ACS relative to k) is contributed. Therefore, $\langle \vec{v}_C \rangle$ represents the clock's velocity relative to the ACS. It is shown in Fig. (16).

(1.2) The velocity of the Artemis rocket relative to the ACS is estimated:

In the Artemis I mission, the rocket needed ca. $t = 5\,\text{days}$ from Earth to the Moon. The distance is ca. $d = 380\,000$ km. Consequently, the speed relative to Earth is estimated by

$$v_{rocket,\underline{\oplus}} = \frac{d}{t} = 880\,\frac{\text{m}}{\text{s}} \text{ and}$$
$$\vec{v}_{rocket,\underline{\oplus}} = -\vec{e}_x \cdot v_{rocket,\underline{\oplus}}. \quad (176)$$

Earth's velocity relative to SCI is $\vec{v}_{\oplus,\underline{SCI}} = \vec{e}_y \cdot 29800\,\frac{\text{m}}{\text{s}}$. Thus, the rocket's velocity relative to Sun is

$$\vec{v}_{rocket,\underline{SCI}} = \vec{v}_{rocket,\underline{\oplus}} + \vec{v}_{\oplus,\underline{SCI}}$$
$$= -\vec{e}_x \cdot 880\,\frac{\text{m}}{\text{s}} + \vec{e}_y \cdot 29800\,\frac{\text{m}}{\text{s}}. \quad (177)$$

Thence, the rocket's velocity relative to the ACS is

$$\vec{v}_{rocket,\underline{ACS}} = \vec{v}_{rocket,\underline{SCI}} - \vec{v}_{ACS,\underline{SCI}} \text{ with}$$
$$\vec{v}_{ACS,\underline{SCI}} = \vec{e}_y \cdot v_{ACS,\underline{SCI}}. \quad (178)$$

It provides the time difference

$$\delta t_{kin,frac} = -\frac{\vec{v}^2_{rocket,\underline{ACS}}}{2c^2}. \quad (179)$$

(2) $\odot$-☾-$\oplus$-triangle:

In this trajectory model, Sun, Moon and Earth form a triangle with a right angle at Earth, see Fig. (15).

The journey takes place at the straight line from Earth to the Moon. For each point P of that straight line, the velocity of the ACS, $\vec{v}_{ACS,\underline{SCI}}$ is derived:

(2.1) The velocity of the ACS, $\vec{v}_{ACS,\underline{SCI}}$, relative to the SCI is equal to the expectation value $\langle \vec{v}_C \rangle$ of a clock in Eq. (156).

(2.2) The velocity of the Artemis rocket relative to the ACS is estimated:

$$v_{rocket,\underline{\oplus}} = 880\,\frac{\text{m}}{\text{s}} \text{ and}$$
$$\vec{v}_{rocket,\underline{\oplus}} = \vec{e}_y \cdot v_{rocket,\underline{\oplus}}. \quad (180)$$

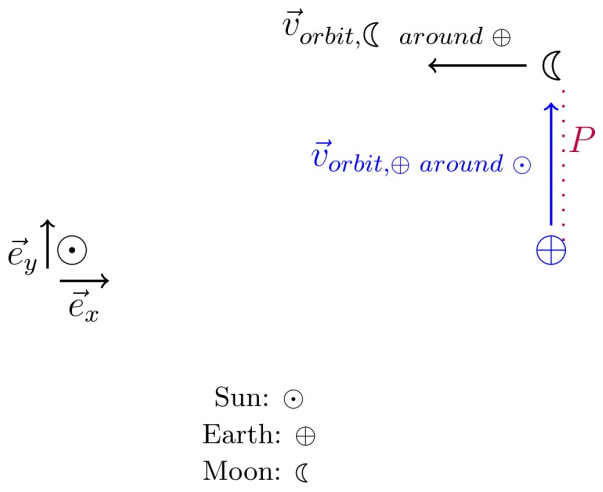

Figure 15: A possible journey from Earth to the Moon is sketched. Thereby, a constellation is investigated with Sun, Earth and Moon forming a triangle with a right angle at Earth.

Earth's velocity relative to SCI is $\vec{v}_{\oplus,\underline{SCI}} = \vec{e}_y \cdot 29800\,\frac{\text{m}}{\text{s}}$. So, the rocket's velocity relative to Sun is

$$\vec{v}_{rocket,\underline{SCI}} = \vec{v}_{rocket,\underline{\oplus}} + \vec{v}_{\oplus,\underline{SCI}}$$
$$= \vec{e}_y \cdot 880\,\frac{\text{m}}{\text{s}} + \vec{e}_y \cdot 29800\,\frac{\text{m}}{\text{s}}. \quad (181)$$

The rocket's velocity relative to the ACS (Eq. 178 and the resulting time difference in Eq. (179) are used.

11.2 Prediction

Two possible constellations of the Sun Earth Moon system are considered, see section (11.1):

(1) $\odot$-☾-$\oplus$-line:

In this constellation, Sun, Moon and Earth are in a straight line, see Fig. (14).

For each point P at that journey, the velocity of the ACS relative to the SCI is presented in Fig. (16). At Earth and at the Moon, the ACS is at these celestial bodies. Consequently, the speed of the ACS, $v_{ACS,\underline{SCI}}$, is approximately equal to the speed $v \approx 29200\,\frac{\text{m}}{\text{s}}$ of these celestial bodies relative to Sun.

In contrast, between Earth and the Moon, close to the Moon, the gravitational field of Sun dominates. Consequently, the ACS moves predominantly with Sun. I. e. the speed of the ACS, $v_{ACS,\underline{SCI}}$, is relatively small.

The fluctuation of the kinematic time difference in Fig. (18) at the ACS is relatively small compared to the kinematic time difference of the rocket, see Fig. (17). Consequently, these fluctuations are not very essential at an Artemis journey from Earth to the Moon.

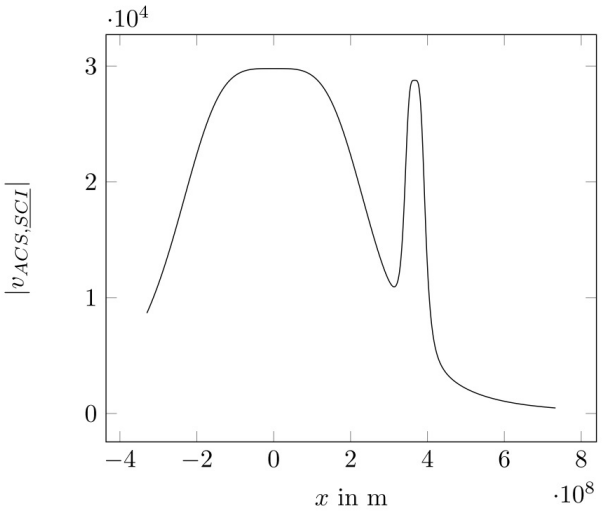

Figure 16: Earth Moon System: Speed $|v_{ACS,\underline{SCI}}|$ of the ACS relative to the Sun Centered Inertial (SCI) system as a function of the location x with $x = 0$ at Earth. At each celestial body, there is a local maximum. The GCRS and the Lunar Centric Celestial Reference system (LCRS), see Kopf (2023), are marked by the high speeds relative to the BCRS.

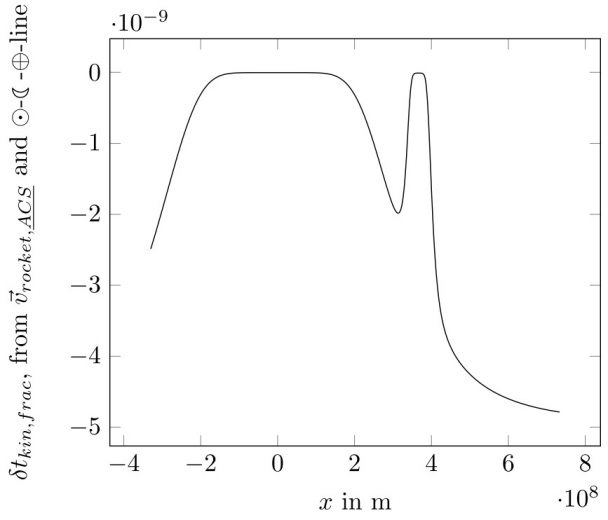

Figure 17: The kinematic fractional time difference $\delta t_{kin,frac}$ as a function of the location x at the Artemis journey from Earth to the Moon in Fig. (14).

(2) ☉-☾ -⊕-triangle:

In this trajectory model, Sun, Moon and Earth form a triangle with a right angle at Earth, see Fig. (15). The resulting kinematic fractional time difference is shown in Eq. (19). It is similar to the time difference in Fig. (17) of constellation (1) in Fig. (14). Therefore, in principle, the interpretation is the same in both cases.

In general, the kinematic time dilation $\delta t_{kin,frac}$ of the rocket predicted here can be tested at a real Artemis journey. Thereby, the real constellation of Sun, Earth and Moon as well as the precise route and schedule of velocities should be used for a precise comparison. The time evolution of the kinematic time dilation $\delta t_{kin,frac}$ of the rocket will in principle be similar to those in Figs. (17 and 19).

12 Applications to geoinformatics

Geoinformatics is an essential tool for the investigation of systems at Earth, planets and space, see Mandla (2025), Carmesin (2025c), Carmesin (2025d). Accordingly, geoinformatics has many methods and applications, see e. g. the textbook Lange (2023).

The purpose of the present investigation is to analyze possible consequences of the above achieved results for geoinformatics. An example is the prediction about the Artemis Moon mission in section (11). Similar consequences will be derived[4].

Physics implies limits about the measurement of data in geoinformatics. In the context of the above investigations, such limits are analyzed:

(1) Screening:

Among the four fundamental interactions, gravity is the only interaction that is not screened. Consequently, gravity is especially adequate for investigations of objects, processes or events inside Earth. These include resources, ore, water, continental drift, early indications of future Earth quakes, early indications for volcanic eruptions.

As gravity modifies the measurable kinematic and gravitational time differences, clocks are essential tools in this context. As gravity curves space, also light can be a useful tool in this field, see e. g. Carmesin (2025h).

(2) Resolution:

An atomic lattice clock can have a fractional time difference of $|\delta t_{frac}| < 10^{-18}$, see e. g. Hinkley (2013), Müller et al. (2018).

However, the measured fractional time difference δt_{frac} is the sum of the kinematic fractional time difference and the gravitational fractional time differ-

[4]It would be beyond the scope of the present investigation to apply these consequences to existing data sets systematically, or to apply these consequences to current measurement tools. Such an application has been developed in Carmesin (2025f,g,h).

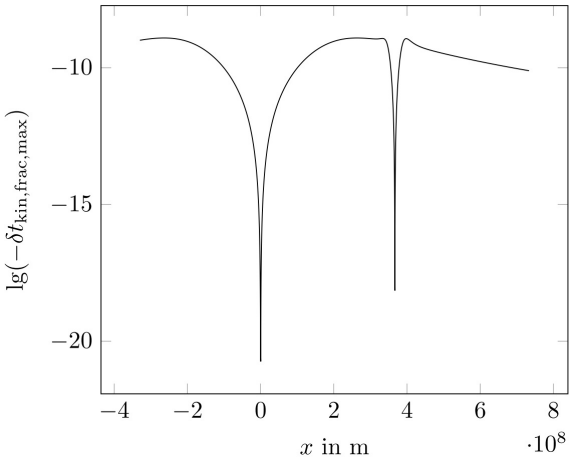

Figure 18: Time fluctuations in the Earth Moon system are shown for the journey in Fig. (14): Logarithm with basis 10 of the negative maximal kinematic time difference $\delta\tau_{\text{kin,frac,min}} = \frac{\langle v^2\rangle - \langle v\rangle^2}{2c^2}$ as a function of the location x with $x = 0$ at Earth. At each planet, there is a local minimum surrounded by two local maxima of that logarithm.

ence:

$$\delta t_{frac} = \delta t_{kin,frac} + \delta t_{grav,frac} \tag{182}$$

Thereby, the gravitational fractional time difference provides valuable information about the gravitational potential, see e. g. Müller et al. (2018), Grotti et al. (2024), Carmesin (2025c).

As a consequence, it is necessary to determine the kinematic fractional time difference, in order to obtain the gravitational fractional time difference:

$$\delta t_{grav,frac} = \delta t_{frac} - \delta t_{kin,frac} \tag{183}$$

For this purpose, the absolute zero of the kinematic fractional time difference $\delta t_{kin,frac}$ discovered here is a very important tool: It provides a universal zero as a reference. With it, deviations can be measured and mapped, similar to the mapping of magnetic variation or magnetic deviation.

The measurement of $\delta t_{kin,frac}$ can be achieved on the basis of the ACS: In many cases, the velocity $\vec{v}_{ACS}$ can be determined with help of the relation to the gravitational field derived here. With it, the velocity $\vec{v}_{C,ACS}$ of a clock C relative to the ACS can be measured, for instance with help of the Doppler effect. With it, the kinematic fractional time difference $\delta t_{kin,frac}$ can be measured at a very high precision.

Thereby, variations of the kinematic time dilation as a function of the locations of nearby celestial bodies can be predicted and used for corrections, see Figs. (16 and 18).

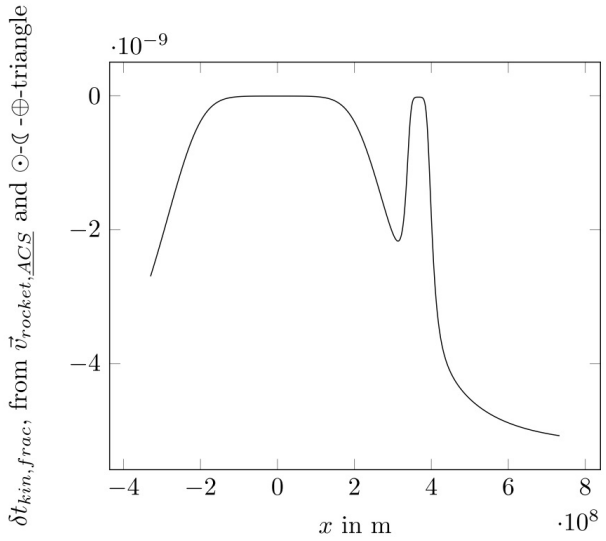

Figure 19: The kinematic fractional time difference $\delta t_{kin,frac}$ as a function of the location x at the Artemis journey from Earth to the Moon, whereby the Moon is located in the $\vec{e}_y$ direction from Earth, see Fig. (15).

Similarly, quantum fluctuations of time differences can be included in the analysis. Hereby, such time differences can be reduced by averaging the time during a time interval τ. This reduces the relative error by the factor $\sqrt{\tau}$, see e. g. Hinkley (2013), Bandhi (2023).

Including these results and methods should improve the interpretation of the values measured with clocks, as these values still include empirically observable deviations from more precise geodetically measured values, see e. g. Grotti et al. (2024), Carmesin (2025c).

In each precise time measurement, the kinematic time difference $\delta t_{kin,frac}$ should be included, as at a relative error of measurement of 10^{-18}, it corresponds to the following speed

$$v = \sqrt{2c^2|\delta t_{frac}|} = 42\ \frac{\text{cm}}{\text{s}}, \tag{184}$$

this is a very small velocity, which can easily occur relative to the ACS. For comparison, at Earth's equator, a clock has a speed relative to the ACS of $465\ \frac{\text{m}}{\text{s}}$.

When the kinematic time difference is subtracted and the gravitational time difference is obtained with the error of measurement of 10^{-18}, it can provide the height at the following error of measurement:

$$\Delta h = \frac{|\delta t_{grav,frac}| \cdot c^2}{g} = 9.2\ \text{mm}. \tag{185}$$

Hereby, the gravitational potential $\Delta\Phi$ and its relation

to the gravitational fractional time difference

$$\delta t_{grav,frac} = \frac{\Delta\Phi}{c^2} = \frac{-g \cdot h}{c^2} \tag{186}$$

have been used.

The above high accuracies achieved by optical atomic lattice clocks illustrate the need of a fundamental understanding and evaluation of kinematic time differences for up to date applications in geoinformatics.

13 Hypothetic deductive method II

The hypothetic deductive method outlined in section (6.1) is used in this paper. Hypotheses that are founded by very reliable observations are used as a basis.

Therefrom, new results are deduced. The deduced results are compared with respective empirical findings, in this section. For on overview of the path of derivations see Fig. (20).

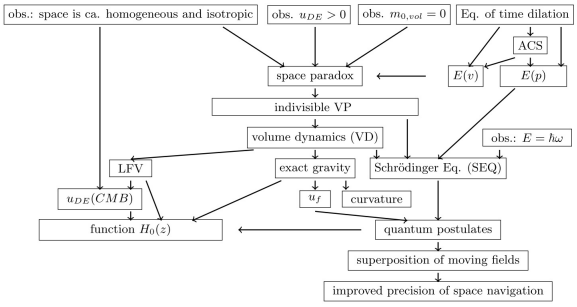

Figure 20: The path of derivations in this paper is represented by this cognitive map.

The quantum postulates are deduced here and confirmed by many observations, see e. g. Ballentine (1998), Scheck (2013).

Laws of gravity are deduced here and confirmed by many observations, see e. g. Tipler and Llewellyn (2008), Landau and Lifschitz (1960).

The curvature of space in the vicinity of a mass is derived. This is confirmed by observation, see e. g. Hobson et al. (2006).

For the vicinity of Earth, the ACS is shown to be the ECI. This is confirmed by observation, see Starker et al. (1985), Carmesin (2025c), Soffel (2003).

For the places in the planetary system that are far away from celestial bodies except Sun, the ACS is shown to be the BCRS or the SCI. This is confirmed by observation, see Soffel (2003).

For a path from Earth to the Moon, the expectation value of the velocity $\langle \vec{v}_{ACS,\underline{SCI}} \rangle$ is deduced as a prediction.

For a path from Earth to the Moon, the expectation value $\langle \delta t_{kin,frac,max} \rangle$ is deduced as a prediction.

For a path in the planetary system, the expectation value $\langle \delta t_{kin,frac,max} \rangle$ is deduced as a prediction.

For the time evolution of the universe since the Big Bang until today, the expectation value $\langle \delta t_{kin,frac,max} \rangle$ is deduced as a prediction in principle.

14 Conclusion

Problem of finding the adequate coordinate system (ACS): The International Astronomical Union (IAU) proclaimed the problem of finding an ACS for the description of space and time in nature Soffel (2003).

Critical discussion of an ACS: A coordinate system is a tool for the coordination of partial quantities. For instance, the quantity length x in the $\vec{e}_x$ direction and the quantity length y in the orthogonal $\vec{e}_y$ direction are coordinated to the length $r = \sqrt{x^2 + y^2}$ in the radial direction, according to the theorem of Pythagoras. This theorem describes adequately characteristics of flat space in nature. More generally, the mutually orthogonal direction vectors $\vec{e}_x$, $\vec{e}_y$ and $\vec{e}_z$ can be used in order to represent the properties of three-dimensional flat space in nature adequately.

More generally, space and time can be coordinated in a Minkowski space Minkowski (1908) with mutually orthogonal direction vectors $\vec{e}_t = \vec{e}_{x_0}$, $\vec{e}_x$, $\vec{e}_y$ and $\vec{e}_z$, in order to represent the properties of four-dimensional flat spacetime in nature in a partially adequate manner. However, the twin paradox Langevin (1911), and additionally, the problem of finding an ACS, see Soffel (2003), indicate that the role of the translatory velocity of the coordinate system must be considered in an adequate manner. Moreover, the Foucault pendulum Foucault (1851) shows that the ACS cannot have an arbitrary rotation.

Accordingly, an ACS is a tool for the precise characterization of the properties of space and time in nature in an adequate manner.

Similarly, a spectrum is an adequate tool in order to describe light in nature, as the spectrum includes the wavelengths, the corresponding rainbow that we see, and the energy spectrum of quanta of light Planck (1900). As a first step, Foucault discovered that the adequate coordinate system cannot rotate in an arbitrary manner Foucault (1851).

Discovery of the ACS: Here, the ACS is discovered by two independent methods: observation and derivation. Thereby, for each point in the universe, the velocity of the ACS is derived in a uniquely determined manner. Thereby, for each point P in the universe,

and for each object C near P, the kinematic time difference of C, the velocity $\vec{v}_{C,\underline{ACS}}$ of C relative to the ACS, the kinetic energy and the relativistic energy $E = E_0/\sqrt{1 - \vec{v}^2_{C,\underline{ACS}}/c^2}$ are derived in a uniquely determined manner. Especially important is the case, in which C is at rest in the ACS, $\vec{v}_{C,\underline{ACS}} = 0$. In that case, the kinematic time difference is zero, everywhere in the universe. Consequently, this represents the absolute zero of the kinematic time difference, of the motion and of the kinetic energy. This holds in non - quantized physics or classical physics. More generally, there occur quantum fluctuations of $\vec{v}_{C,\underline{ACS}}$.

Discovery of the indivisible parts of space, based on the ACS: Based on the above relativistic energy, for space in nature, the space paradox, see Carmesin (2025a), is derived. As a consequence, space in nature is a stochastic average of indivisible portions. A portion of volume in nature or of space in nature is called volume portion (VP).

Discovery of the dynamics of volume portions: Based on mathematics, the dynamics of VPs is derived Carmesin (2021b).

Discovery of the Schrödinger equation (SEQ): Based on the dynamics of VPs, the SEQ and a generalized Schrödinger equation (GSEQ) are derived. According to the Higgs mechanism, volume can make a phase transition to mass. Consequently, the derived SEQ is derived for mass as well. Moreover, the GSEQ describes electromagnetic radiation additionally Carmesin (2024a, 2021c, 2022c). In this manner, the following emerges from the ACS: the indivisible volume portions, their description by the volume dynamics, their description by the GSEQ, the description of mass (a transformed version of vacuum or of volume in nature) by the SEQ, and the SEQ in general.

Discovery of gravity and curvature of space and time: Based on the dynamics of VPs, the following is exactly derived, discovered, and (ultimately) emerging from the ACS: the exact gravitational potential as an average of relative additional volume of indivisible VP multiplied by $-c^2$, the corresponding exact gravitational field, the curvature of spacetime in the same averaged (or non - quantized) manner.

Discovery of the quantum postulates: Based on the dynamics of VPs, on the SEQ, and on the emergent gravity, the quantum postulates are derived, explained, and (ultimately) emerging from the ACS, see Carmesin (2022b), Carmesin (2022a). Consequently, these so-called quantum postulates are no longer postulates, but they are derived, explained, and founded rules of physics. Therefore, the ACS and the VPs imply quantum physics as well as gravity, so that a bridge between quanta and gravity emerges, which can be interpreted as a unification of gravity and quanta.

Prediction of the ACS: Based on the derived so-called quantum postulates, for each point in the universe, the velocity of the ACS is derived. This completes the solution of the problem proclaimed by the IAU, the problem to find an ACS. Here, a test of this prediction is elaborated: The kinematic time difference can be measured onboard the spacecraft of the Artemis mission on its way from Earth to the Moon.

Further predictions and evidence: Further evidence for the theory of VPs has been achieved as follows: Firstly, the energy density of cosmological vacuum or of space or of dark energy has been derived, see Carmesin (2021b), Carmesin (2024c), Carmesin (2024a), Carmesin (2025e). Secondly, the Hubble tension has been explained and the value of the Hubble constant H_0 as a function of the redshift z has been derived and predicted, see e. g. Carmesin (2021b), Carmesin (2024b), Carmesin (2024a), Carmesin (2021a), Carmesin (2025b), Carmesin (2025e). These two derived results are in precise accordance with observation, and thereby no fit has been executed, and no postulate or unfounded hypothesis has been proposed or used.

Application to geoinformatics: Coordinate systems are an essential tool of geoinformatics Lange (2023). The ACS clearly improves the present - day coordinate systems. This can clearly improve the accuracy of measurements, data, results and products in geoinformatics (see section 12).

Acknowledgements: I thank Matthias and Christian Carmesin as well as Victorio Lato for interesting discussions. I am especially grateful to I. Carmesin for many stimulating discussions and for carefully reading the manuscript.

References:

[1]. Aad, G. e. a. (2012). Observation of a new particle in the search for the Standard Model Higgs boson with the ATLAS detector at the LHC. Phys. Lett. B, 716:1.

[2]. Abbott, B. P. e. a. (2016). Observation of gravitational waves from a binary black hole merger. Phys. Rev. Lett., 116:1–16.

[3]. Archimedes (1897). The Sand-Reckoner (230 BC), translated by Heath. Cambridge University Press, Cambridge.

[4]. Aristarchos (270 BC). Aristarchos of Samos – the Ancient Copernicus, translated by T. L. Heath (1913). Clarendon Press, Oxford.

[5]. Ashby, N. (2003). Relativity and the global positioning system. Living Rev. Relativity, 6:1–42.

[6]. Aspect, A., Grangier, P., & Roger, G. (1982). Experimental realization of the Einstein–Podolski–Rosen–Bohm Gedankenexperiment. Phys. Rev. Lett., 49:91–94.

[7]. Ballentine, L. E. (1998). Quantum Mechanics. World Scientific Publishing, London & Singapore.

[8]. Bandhi, T. N. (2023). A comprehensive overview of atomic clocks and their applications. BEMS Reports, 92:1–10.

[9]. Blanchet, L. (2024). Post-Newtonian theory for gravitational waves. Living Reviews in Relativity, 27(4):1–292.

[10]. Blokhintsev, D. I., & Galperin, F. M. (1934). Neutrino hypothesis and conservation of energy. Pod Znamenem Marxisma, 6:147–157.

[11]. Bose, S. (1924). Plancks Gesetz und Lichtquantenhypothese. Z. f. Physik, 26:178–181.

[12]. Brockhaus, T. (1998). Brockhaus, die Enzyklopädie. Brockhaus GmbH, Leipzig–Mannheim, 20th ed.

[13]. Burisch, C. et al. (2025). Universum Physik Gesamtband S II. Cornelsen Verlag, Berlin.

[14]. Carmesin, H.-O. (2017). Vom Big Bang bis heute mit Gravitation. Verlag Dr. Köster, Berlin.

[15]. Carmesin, H.-O. (2018). Entstehung der Raumzeit durch Quantengravitation. Verlag Dr. Köster, Berlin.

[16]. Carmesin, H.-O. (2019). Die Grundschwingungen des Universums. In Universe: Unified from Microcosm to Macrocosm, Vol. 1, pp. 1–226.

[17]. Carmesin, H.-O. (2020). Wir entdecken die Geschichte des Universums. In Universe: Unified from Microcosm to Macrocosm, Vol. 2.

[18]. Carmesin, H.-O. (2021a). Cosmological and Elementary Particles Explained by Quantum Gravity. Vol. 5, pp. 1–198.

[19]. Carmesin, H.-O. (2021b). Quanta of Spacetime Explain Observations. Vol. 4, pp. 1–2743.

[20]. Carmesin, H.-O. (2021c). The Elementary Charge Explained by Quantum Gravity. Vol. 6, pp. 1–149.

[21]. Carmesin, H.-O. (2022a). Explanation of quantum physics by gravity and relativity. PhyDid B, 425–438.

[22]. Carmesin, H.-O. (2022b). Quantum Physics Explained by Gravity and Relativity. Vol. 7, pp. 1–148.

[23]. Carmesin, H.-O. (2022c). The Electroweak Interaction Explained. Vol. 8, pp. 1–168.

[24]. Carmesin, H.-O. (2023). Geometric and Exact Unification of Spacetime. Vol. 10, pp. 1–320.

[25]. Carmesin, H.-O. (2024a). How Volume Portions Form and Found Light. Vol. 11, pp. 1–320.

[26]. Carmesin, H.-O. (2024b). Students analyze the impact of the H_0 tension. PhyDid B, 405–412.

[27]. Carmesin, H.-O. (2024c). Students learn to derive the energy density of volume. PhyDid B, 35–42.

[28]. Carmesin, H.-O. (2024d). Students learn to derive universal properties of gravitons. PhyDid B, 413–421.

[29]. Carmesin, H.-O. (2025a). A fundamental path to quantum physics. PhyDid B, 337–345.

[30]. Carmesin, H.-O. (2025b). A fundamental solution of the Hubble tension. Foundations, preprints.org.

[31]. Carmesin, H.-O. (2025c). Construction of a physically adequate coordinate system. Journal of Geosciences, 1(1):01–12.

[32]. Carmesin, H.-O. (2025d). Derivation of a physically adequate coordinate system from space. Elsevier SSRN.

[33]. Carmesin, H.-O. (2025e). On the Dynamics of Time, Space and Quanta. Vol. 12, pp. 1–231.

[34]. Carmesin, H.-O. (2025f). Patent application April AKZ 102025001259.4.

[35]. Carmesin, H.-O. (2025g). Patent application August AKZ 102025002783.4.

[36]. Carmesin, H.-O. (2025h). Patent application September AKZ 102025003071.1.

[37]. Casimir, H. (1948). On the attraction between two perfectly conducting plates. Proc. KNAW, 51:793–795.

[38]. Chandrasekhar, S. (1965). Post-Newtonian equations of hydrodynamics. Astrophysical Journal, 142:1488–1512.
[39]. Chatrchyan, S. e. a. (2012). Observation of a new boson at 125 GeV. Phys. Lett. B, 716:30.
[40]. Ciufolini, I., & Pavlis, E. C. (2004). Lense–Thirring effect. Nature, 431:958–960.
[41]. Clauser, J. F., & Horne, M. A. (1974). Experimental consequences of objective local theories. Phys. Rev. D, 10:526–535.
[42]. Condon, J. J., & Matthews, A. M. (2018). ΛCDM cosmology for astronomers. PASP, 130.
[43]. Contarini, S. et al. (2024). Voids and cosmology tensions. A&A, 682:A20.
[44]. DFVLR (1985). D-1 Report: The First German Spacelab Mission. NASA.
[45]. Dyson, F. W., Eddington, A. S., & Davidson, C. (1920). Deflection of light by the sun. Phil. Trans. R. Soc. A, 220:291–333.
[46]. Einstein, A. (1905). Zur Elektrodynamik bewegter Körper. Annalen der Physik, 17:891–921.
[47]. Einstein, A. (1915). Die Feldgleichungen der Gravitation. Sitzungsberichte, 844–847.
[48]. Einstein, A. (1916). Grundlage der allgemeinen Relativitätstheorie. Annalen der Physik, 49:769–822.
[49]. Einstein, A. (1917). Kosmologische Betrachtungen. Sitzungsberichte, 142–152.
[50]. Formichella, V. et al. (2021). Galileo satellite clocks. GPS Solutions.
[51]. Foucault, L. (1851). Physical demonstration of the Earth's rotational movement. Comptes Rendus, 32:135–138.
[52]. Friedmann, A. (1922). Über die Krümmung des Raumes. Z. f. Physik, 10:377–386.
[53]. Galbany, L. e. a. (2023). Updated Hubble constant measurement. A&A, 679:1–26.
[54]. Galileo, G. (1638). Dialogues Concerning Two New Sciences. Elzevirii, Leiden.
[55]. Griffiths, D. J. (1994). Introduction to Quantum Mechanics. Prentice Hall.
[56]. Grotti, J. et al. (2024). Long-distance chronometric levelling. Phys. Rev. Applied, 21.
[57]. Guericke, O. v. (1672). Experimenta Nova Magdeburgica. Amsterdam.
[58]. Hacking, I. (1983). Representing and Intervening. Cambridge University Press.
[59]. Heisenberg, W. (1927). Über den anschaulichen Inhalt der Quantenmechanik. Z. f. Physik, 43:172–198.
[60]. Higgs, P. W. (1964). Broken symmetries. Phys. Lett., 132–133.
[61]. Hilbert, D. (1915). Die Grundlagen der Physik. Nachrichten Göttingen.
[62]. Hilbert, D., Nordheim, L., & von Neumann, J. (1928). Grundlagen der Quantenmechanik. Math. Ann., 395–407.
[63]. Hinkley, N. e. a. (2013). Atomic clock with 10^{-18} instability. Science, 341:1215–1218.
[64]. Hobson, M. P. et al. (2006). General Relativity. Cambridge University Press.
[65]. Hoskin, M. (1999). The Cambridge Concise History of Astronomy. CUP.
[66]. Huterer, D., & Turner, M. S. (1999). Dark energy via supernovae. Phys. Rev. D, 60.
[67]. Joeris, K. et al. (2025). Partial gravity platform. Rev. Sci. Instr., 96.
[68]. Karttunen, H. et al. (2007). Fundamental Astronomy. Springer.
[69]. Kelvin, W. (1848). Absolute thermometric scale. Philosophical Magazine.
[70]. Kim, K. et al. (2023). Lattice light shift evaluation. PRL, 130.
[71]. Kopf, A. (2023). Lunar celestial reference system. Bulletin of the AAS.
[72]. Kumar, A. (2018). Fundamentals of Quantum Mechanics. CUP.
[73]. Landau, L., & Lifshitz, E. (1960). Mechanics. Pergamon Press.
[74]. Landau, L., & Lifshitz, E. (1965). Quantum Mechanics. Pergamon Press.
[75]. Landau, L., & Lifshitz, E. (1971). Classical Theory of Fields. Pergamon Press.
[76]. Landau, L., & Lifshitz, E. (1976). Mechanics. Pergamon Press.
[77]. Landau, L., & Lifshitz, E. (1980). Statistical Physics. Pergamon Press.
[78]. Lange, D. N. (2023). Geoinformatics in Theory and Practice. Springer.
[79]. Langevin, P. (1911). L'évolution de l'espace et du temps. Scientia.
[80]. Lavery, J. E. (1972). Relativistic time corrections. NASA TN D-6681.
[81]. Lee, J. M. (1997). Riemannian Manifolds. Springer.
[82]. Lemaître, G. (1927). Un univers homogène. Ann. Soc. Sci. Bruxelles, A47.
[83]. Lense, J., & Thirring, H. (1918). Eigenrotation effects. Z. f. Physik, 19.
[84]. Liu, T., & Liao, K. (2024). Model-independent H_0. MNRAS, 528.

[85]. Losada, V. et al. (2025). Measuring PPN parameters. A&A, 694.
[86]. Ma, X.-S. et al. (2012). Quantum teleportation. Nature, 489.
[87]. Mandal, A., & Nadkarni-Ghosh, S. (2020). Early dark energy. MNRAS, 498.
[88]. Mandla, V. e. a. (2025). Geoinformatics trends. Front. Earth Sci., 13.
[89]. Maxwell, J. C. (1865). Electromagnetic field theory. Phil. Trans. R. Soc., 155.
[90]. Minkowski, H. (1908). Raum und Zeit. JDMV, 18.
[91]. Moore, T. A. (2013). A General Relativity Workbook.
[92]. Müller, J. et al. (2018). High performance clocks. Space Sci. Rev., 214.
[93]. NASA (2022). NASA Lunar Programs. GAO.
[94]. Navas, S. et al. (2024). Review of particle physics. Phys. Rev. D, 110.
[95]. Newton, I. (1687). Principia Mathematica. London.
[96]. Niiniluoto, I. et al. (2004). Handbook of Epistemology. Springer.
[97]. Peebles, P. J. E., & Ratra, B. (1988). Cosmological constant. ApJ, 325.
[98]. Perlmutter, S. et al. (1998). Accelerating universe. Nature, 391.
[99]. Peters, P. C. (1981). Gravitational field energy. Am. J. Phys., 49.
[100]. Planck, M. (1900). Energy distribution law. Verh. DPG, 2.
[101]. Planck Collaboration (2020). Planck 2018 results. A&A.
[102]. Popper, K. (1935). Logik der Forschung. Springer.
[103]. Popper, K. (1974). Objektive Erkenntnis. Hoffmann & Campe.
[104]. Pound, R. V., & Rebka, G. A. (1960). Weight of photons. PRL, 4.
[105]. Redlich, O. (1970). Intensive and extensive properties. J. Chem. Educ., 2.
[106]. Riess, A. G. et al. (2000). Accelerating universe tests. ApJ, 536.
[107]. Riess, A. G. et al. (2022). Local Hubble constant. ApJL, 934.
[108]. Sakurai, J. J., & Napolitano, J. (1994). Modern Quantum Mechanics.
[109]. Sardin, G. (2001). Absolute speed measurement. Europhys. Lett., 53.
[110]. Scheck, F. (2013). Quantum Physics. Springer.
[111]. Schrödinger, E. (1926). Eigenvalue problem. Ann. Phys., 81.
[112]. Schwarzschild, K. (1916). Gravitational field. Sitzungsberichte.
[113]. Shech, E. (2023). Idealizations in Physics. CUP.
[114]. Smoot, G. F. (2007). Nobel lecture. Rev. Mod. Phys., 79.
[115]. Soffel, M. e. a. (2003). IAU 2000 resolutions. AJ, 126.
[116]. Song, J. e. a. (2002). Idealization in physics education. Elsevier.
[117]. Starker, S. et al. (1985). NAVEX D1 mission. Washington DC.
[118]. Starker, S. et al. (1982). NAVEX atomic clocks.
[119]. Stephani, H. (1980). Allgemeine Relativitätstheorie.
[120]. Teschl, G. (2014). Mathematical Methods in QM. AMS.
[121]. Tipler, P. A., & Llewellyn, R. A. (2008). Modern Physics.
[122]. Unsöld, A., & Baschek, B. (1999). Der neue Kosmos.
[123]. van der Waals, J. D. (1873). Continuity of gas and liquid states.
[124]. Wiggins, S. (2003). Nonlinear Dynamical Systems. Springer.
[125]. Will, C. M. (2014). GR and experiment. Living Rev. Relativity, 17.
[126]. Workman, R. L. et al. (2022). Review of particle physics. PTEP, 083C01.
[127]. Yang, Z. (2014). Post-Newtonian Inspirals. PhD Thesis.
[128]. Zeilinger, A. et al. (1988). Neutron slit experiments. Rev. Mod. Phys., 60.
[129]. Zeldovich, Y. B. (1968). Cosmological constant. Sov. Astron., 11.
[130]. Zeldovich, Y. B. et al. (1982). Giant voids. Nature, 300.
[131]. Zogg, J.-M. (2009). GPS Essentials. u-blox AG.